Received: 30 March 2021 | Revised: 25 October 2021 | Accepted: 29 October 2021

DOI: 10.1002/JLB.5HI0321-179RR

HIGHLIGHTED ARTICLE

JLB JOURNAL OF LEUKOCYTE BIOLOGY

Specific innate immune cells uptake fetal antigen and display homeostatic phenotypes in the maternal circulation

Marcia Arenas-Hernandez[1,2] | Roberto Romero[1,3,4,5,6] | Meyer Gershater[1,2] | Li Tao[1,2] | Yi Xu[1,2] | Valeria Garcia-Flores[1,2] | Errile Pusod[1,2] | Derek Miller[1,2] | Jose Galaz[1,2] | Kenichiro Motomura[1,2] | George Schwenkel[1,2] | Robert Para[1,2] | Nardhy Gomez-Lopez[1,2,7]

[1] Perinatology Research Branch, Division of Obstetrics and Maternal-Fetal Medicine, Division of Intramural Research, *Eunice Kennedy Shriver* National Institute of Child Health and Human Development, National Institutes of Health, U. S. Department of Health and Human Services, Bethesda, Maryland, and Detroit, Michigan, USA

[2] Department of Obstetrics and Gynecology, Wayne State University School of Medicine, Detroit, Michigan, USA

[3] Department of Obstetrics and Gynecology, University of Michigan, Ann Arbor, Michigan, USA

[4] Department of Epidemiology and Biostatistics, Michigan State University, East Lansing, Michigan, USA

[5] Center for Molecular Medicine and Genetics, Wayne State University, Detroit, Michigan, USA

[6] Detroit Medical Center, Detroit, Michigan, USA

[7] Department of Biochemistry, Microbiology, and Immunology, Wayne State University School of Medicine, Detroit, Michigan, USA

Correspondence
Nardhy Gomez-Lopez, Department of Obstetrics and Gynecology, Wayne State University, School of Medicine, Perinatology Research Branch, NICHD/NIH/DHHS, 275 E Hancock St, Detroit, Michigan 48201 USA.
Email: nardhy.gomez-lopez@wayne.edu; ngomezlo@med.wayne.edu

Abstract

Pregnancy represents a period when the mother undergoes significant immunological changes to promote tolerance of the fetal semi-allograft. Such tolerance results from the exposure of the maternal immune system to fetal antigens (Ags), a process that has been widely investigated at the maternal-fetal interface and in the adjacent draining lymph nodes. However, the peripheral mechanisms of maternal-fetal crosstalk are poorly understood. Herein, we hypothesized that specific innate immune cells interact with fetal Ags in the maternal circulation. To test this hypothesis, a mouse model was utilized in which transgenic male mice expressing the chicken ovalbumin (OVA) Ag under the beta-actin promoter were allogeneically mated with wild-type females to allow for tracking of the fetal Ag. Fetal Ag-carrying Ly6G$^+$ and F4/80$^+$ cells were identified in the maternal circulation, where they were more abundant in the second half of pregnancy. Such innate immune cells displayed unique phenotypes: while Ly6G$^+$ cells expressed high levels of MHC-II and CD80 together with low levels of pro-inflammatory cytokines, F4/80$^+$ cells up-regulated the expression of CD86 as well as the anti-inflammatory cytokines IL-10 and TGF-β. In vitro studies using allogeneic GFP$^+$ placental particles revealed that maternal peripheral Ly6G$^+$ and F4/80$^+$ cells phagocytose fetal Ags in mid and late murine pregnancy. Importantly,

Abbreviations: GFP, green fluorescent protein; HLA, human leukocyte Ag; NET, neutrophil extracellular trap; OVA, ovalbumin; PP, postpartum; ROS, reactive oxygen species; STBM, syncytiotrophoblast-derived microparticles.

cytotrophoblast-derived particles were also engulfed in vitro by CD15$^+$ and CD14$^+$ cells from women in the second and third trimester, providing translational evidence that this process also occurs in humans. Collectively, this study demonstrates novel interactions between specific maternal circulating innate immune cells and fetal Ags, thereby shedding light on the systemic mechanisms of maternal-fetal crosstalk.

KEYWORDS
human, innate immune cells, maternal-fetal tolerance, mice, OVA, peripheral blood, pregnancy

1 | INTRODUCTION

Pregnancy represents a period of significant immunological changes in the mother that allow her to tolerate the fetal semi-allograft.[1–5] Among these adaptations, the best-characterized are those that occur at the site of contact between the maternal and fetal tissues, termed the maternal-fetal interface.[6] In this compartment and in the adjoining tissues (e.g., the uterine-draining lymph nodes),[7–14] exposure of the maternal immune system to fetus-derived antigens (Ags) initiates the establishment of tolerance[15–17] by promoting the induction of regulatory T cells (Tregs).[8,18–27] Other mechanisms of maternal-fetal tolerance may include effector T-cell exhaustion[28,29] and the enrichment of the homeostatic immune microenvironment by innate immunoregulatory cells.[30–37] The placenta also contributes to local tolerance by expressing immunomodulatory non-classical MHC molecules (e.g., HLA-G) that inhibit NK cell responses[38–40] as well as inhibitory checkpoint ligands such as PD-L1.[41,42] Together, these and other[4,43] cellular processes mediate the local mechanisms of maternal-fetal tolerance.

An established hallmark of pregnancy is the transfer of fetal cells into the maternal circulation[44–46] (and vice versa[47–50]), a phenomenon termed fetal or maternal microchimerism, respectively. Fetal microchimerism is detected as early as 7 weeks of gestation,[46] and the abundance of such cells (as well as their genetic material) steadily increases throughout pregnancy.[46] Such a process not only participates in the mechanisms of maternal-fetal tolerance[51,52] but can also have long-lasting effects, given that fetal or maternal cells are observed in the circulation of the mother and offspring, respectively, for decades after delivery.[45,47] In addition to fetal cells, the placenta can also release microparticles and exosomes into the maternal circulation, either due to apoptotic turnover or by active secretion.[53–63] Specifically, placenta-derived particles serve as modulators of maternal systemic immune responses[54–56,59,60,64–67] and, similar to fetal cells, their concentrations increase as gestation progresses.[53,56,68] However, the interactions between placenta-derived microparticles and maternal circulating immune cells have not been well explored.

Previous studies have established that the phenotypes and functions of neutrophils and monocytes in the maternal circulation are highly impacted throughout pregnancy.[69–71] Neutrophils from pregnant women exhibit an enhanced state of activation as evidenced by the increased expression of cell surface markers (e.g., CD14 and CD64),[69,70] higher basal intracellular reactive oxygen species (iROS) levels[69,70,72] and reactive oxygen metabolite release,[73] and altered phagocytic activity,[74–76] compared to those from non-pregnant women. Similarly, monocytes from pregnant women display increased cell surface marker expression (e.g., CD11b, CD18, and CD64),[69,70,77,78] greater basal iROS production,[69,70] enhanced cytokine responses,[56,79] and perturbed phagocytic activity,[75,80] compared to those from non-pregnant women. Yet, whether such innate immune cells interact with fetus-derived Ags in the maternal circulation is unknown.

The aim of this study was to investigate whether maternal circulating Ly6G$^+$ cells (i.e., neutrophils) and F4/80$^+$ cells (i.e., monocytes/macrophages) capture fetal Ags throughout gestation. Specifically, we utilized transgenic male mice that express the chicken ovalbumin (OVA) Ag under the beta-actin promoter, which were allogeneically mated with wild-type females to allow for tracking of the fetal Ag.[9,81–83] First, we explored the localization of the fetal Ag in Ly6G$^+$ and F4/80$^+$ cells in the myometrium and periphery as well as their kinetics throughout pregnancy. Second, using flow cytometry, we characterized the phenotypes and cytokine profiles of fetal Ag-carrying Ly6G$^+$ and F4/80$^+$ cells and confirmed their maternal origin. Third, functional in vitro studies were utilized to investigate whether the fetal Ag can be phagocytosed by maternal peripheral Ly6G$^+$ and F4/80$^+$ cells during mid and late murine gestation. Lastly, to demonstrate the translational value of our findings in mice, we performed in vitro studies that utilized maternal peripheral CD15$^+$ cells (i.e., neutrophils) and CD14$^+$ cells (i.e., monocytes) from second- and third-trimester pregnancies to explore whether cytotrophoblast-derived particles can also be engulfed by such innate immune cells.

2 | MATERIALS AND METHODS

2.1 | Mice

C57BL/6-Tg(CAG-OVAL)916Jen/J (Act-mOVA II) (hereafter referred to as B6 CAG-OVA) male, BALB/cByJ (BALB/c) female and male, C57BL/6 female and C57BL/6 male (hereafter referred to as B6 non-CAG-OVA), C57BL/6 Actb-Egfp (GFP$^+$) male, and DBA/2 female mice were purchased from The Jackson Laboratory (Bar Harbor, ME), bred in

the animal care facility at the C.S. Mott Center for Human Growth and Development, Wayne State University, Detroit, MI, and housed under a circadian cycle (light:dark = 12:12 h). Eight- to 12-week-old females were examined daily between 8:00 and 9:00 am for the presence of a vaginal plug, which indicated 0.5 days *post coitum* (dpc). Upon observation of vaginal plugs, female mice were removed from mating cages and housed separately. Pregnancy at 4.5 dpc was confirmed ex vivo by using trypan blue to stain the implantation sites, followed by washing with 1× phosphate-buffered saline (PBS; Fisher Scientific Chemicals, Fair Lawn, NJ). Pregnancy at 10.5 dpc was confirmed by a weight gain of ≥2 g. Postpartum BALB/c females (PP; 48 - 60 h after delivery) were also included in this study. All experiments were approved by the Institutional Animal Care and Use Committee at Wayne State University (Protocol No. A 09-08-12, A 07-03-15, 18-03-0584, and 21-04-3506).

2.2 | Human subjects and clinical specimens

Peripheral blood samples were obtained from women enrolled in research protocols of the Perinatology Research Branch, an intramural program of the *Eunice Kennedy Shriver* National Institute of Child Health and Human Development, National Institutes of Health, U.S. Department of Health and Human Services, Wayne State University (Detroit, MI), Detroit Medical Center (Detroit, MI). The collection and use of human materials for research purposes were approved by the Institutional Review Boards of Wayne State University and the National Institute of Child Health and Human Development. All participating women provided written informed consent prior to sample collection. Samples were obtained from healthy women with a normal pregnancy in the second or third trimester.

2.3 | Hematoxylin and eosin staining of fetal and myometrial murine tissues

Fetuses and the surrounding myometrial tissues were collected from dams at 10.5 dpc, 16.5 dpc, and 18.5 dpc and placed into Tissue Tek OCT freezing medium (Sakura Finetek USA, Inc., Torrance, CA) (n = 3 - 10 each). Sagittal cuts of 16 μm thickness were taken from each fetus. Slices were mounted on slides and fixed with 4% paraformaldehyde (Electron Microscopy Sciences, Hatfield, PA) for 30 minutes (min) at 4°C. Slides were stained with hematoxylin (Thermo Fisher Scientific, Waltham, MA) for 1 min and 10 seconds (s), and immersed in clarifier for 5 s and blueing agent for 20 s, rinsing the slides with distilled water after each step. The slides were then stained with eosin (Thermo Fisher Scientific) for 45 s and dehydrated in a series of alcohol baths and xylene prior to applying a coverslip. All H&E images were taken by using a Vectra Polaris Multispectral Imaging System (PerkinElmer, Waltham, MA, USA) at 4× magnification.

2.4 | Confocal microscopy of fetal and myometrial murine tissues

Fetuses and the surrounding myometrial tissues were collected from dams at 10.5 dpc, 16.5 dpc, and 18.5 dpc and placed into Tissue Tek OCT freezing medium (n = 3 - 10 each). Sagittal cuts of 16 μm thickness were taken from each fetus. Slices were mounted on slides and fixed with 4% paraformaldehyde (Electron Microscopy Sciences) in 1× phosphate-buffered saline (PBS; Life Technologies, Grand Island, NY) for 30 min at 4°C. Slides were then rinsed with 1× PBS (Life Technologies), permeabilized with 0.25% Triton X-100 (Promega Corporation, Madison, WI) for 5 min at room temperature (RT), rinsed again with 1× PBS, and blocked with 5% BSA (Sigma-Aldrich, St Louis, MO) diluted in 1× PBS for 30 min at RT. The primary anti-OVA-FITC (Cat # 200-4233-0101, Rockland Immunochemicals, Inc. Gilbertsville, PA) antibody (Ab) or rabbit IgG-FITC isotype control was added and the slides were incubated for 1 h at RT. The slides were washed with 1× PBS, anti-mouse CD11b-Alexa Fluor 594 Ab (Cat # 101254, BioLegend, San Diego, CA) was added, and the slides were incubated for 30 min at RT. After washing, slides were mounted with ProLong Gold Mounting medium with 4′,6-diamidino-2-phenylindole (DAPI) (Life Technologies). Immunofluorescence was visualized with a Zeiss LSM 780 laser scanning confocal microscope (Carl Zeiss Microscopy, Jena, Germany) at the Microscopy, Imaging, and Cytometry Resources Core of Wayne State University School of Medicine (https://micr.med.wayne.edu/). The 561 nm line of an "in-tune" tunable white laser was used to excite Alexa Fluor 594, the 488 nm line of the tunable white laser to excite FITC, and the 405 nm diode laser to excite DAPI.

2.5 | Cell sorting

Dams at 10.5 dpc and 18.5 dpc were euthanized and peripheral blood was obtained by cardiac puncture (n = 10 each). Peripheral leukocytes were incubated with the CD16/CD32 mAb (FcγIII/II receptor; BD Biosciences, San Jose, CA) followed by staining using anti-mouse CD11b-PE-CF594, anti-mouse Ly6G-APC-Cy7, and anti-mouse F4/80-PE mAbs (BD Biosciences), after which the cell suspensions underwent intracellular staining with either anti-OVA-FITC Ab or rabbit IgG-FITC isotype control. Cells were resuspended in 500 μL of FACS buffer and sorted by using a BD FACSAria cell sorter (BD Biosciences) and BD FACSDiva Software v6.1.3. The sorted $CD11b^+Ly6G^+OVA^+$ or $CD11b^+F4/80^+OVA^+$ cells were then resuspended with 200 μL of FACS buffer [0.1% BSA and 0.05% sodium azide (Fisher Scientific Chemicals) in 1× PBS]. Cytospin slides of sorted cells were prepared using Fisherbrand Superfrost microscope slides (Thermo Fisher Scientific) and a Shandon Cytospin 3 cytocentrifuge (Thermo Fisher Scientific) at 800 rpm for 5 min. After centrifugation, all slides were washed with 1× PBS and the cells were fixed with 4% paraformaldehyde for 20 min. After fixation, the slides were washed with 1× PBS, dried,

and mounted using ProLong Diamond Antifade Mountant with DAPI. Images were obtained with an Olympus BX60 fluorescence microscope at 40× magnification with digital zoom.

2.6 | Leukocyte isolation from the murine maternal circulation and myometrium

2.6.1 | Identification of fetal Ag-carrying immune cells throughout pregnancy and postpartum

Dams mated with B6 CAG-OVA or non-CAG-OVA males were euthanized at 4.5 dpc, 10.5 dpc, 16.5 dpc, 18.5 dpc, and in the postpartum period, and peripheral blood was obtained by cardiac puncture. Non-pregnant females were also included as controls. Myometrial tissues from the implantation sites were collected (n = 2 – 14 each), and images of the uterine horns were taken. Isolation of leukocytes from myometrial tissues was performed as previously described.[84] Briefly, tissues were minced with fine scissors and enzymatically digested with StemPro Cell Dissociation Reagent (Life Techologies) for 35 min at 37°C. Leukocyte suspensions were filtered with a 100-μm cell strainer (Fisherbrand; Fisher Scientific, Fair Lawn, NY) and washed with FACS buffer immediately prior to immunophenotyping.

2.6.2 | Immunophenotyping of fetal Ag-carrying immune cells in mid and late pregnancy

Dams at 10.5 dpc (mid-pregnancy) and 16.5 dpc (late pregnancy) were euthanized and peripheral blood was obtained by cardiac puncture (n = 9 – 12 each). Myometrial tissues from the implantation sites were collected (n = 9 – 11 each). Isolation of leukocytes from myometrial tissues was performed, as previously described.[84] Isolated leukocytes were utilized for immunophenotyping.

2.7 | Immunophenotyping of murine leukocytes

2.7.1 | Identification of fetal Ag-carrying immune cells throughout pregnancy and postpartum

Maternal peripheral blood (150 μL) and leukocyte suspensions from the myometrium were centrifuged at 1250 × g for 10 min at 4°C, and cell pellets were incubated with the CD16/CD32 mAb (FcγIII/II receptor; BD Biosciences) for 10 min, and subsequently incubated with specific fluorochrome-conjugated anti-mouse mAbs (Supplementary Table S1) for 30 min at 4°C in the dark. After washing, the cells were fixed and permeabilized with the BD Cytofix/Cytoperm kit (BD Biosciences) prior to staining with intracellular Abs. For intracellular staining, anti-OVA-FITC Ab or its isotype control (Supplementary Table S1) was added to the cells, which were then incubated for 30 min at 4°C in the dark. Following staining, cells were acquired by using the BD LSRFortessa flow cytometer (BD Biosciences) and FACS-Diva 8.0 software (BD Biosciences). Immunophenotyping included the identification of $CD45^+Ly6G^+OVA^+$ (or $CD45^+Ly6G^+OVA^-$) cells and $CD45^+F4/80^+OVA^+$ (or $CD45^+F4/80^+OVA^-$) cells in the myometrium and peripheral blood. Data were analyzed with FlowJo software v10 (FlowJo, Ashland, OR).

2.7.2 | Immunophenotyping of fetal Ag-carrying immune cells in mid and late pregnancy

Maternal peripheral blood (150 μL) and leukocyte suspensions from the myometrium were stained by using the LIVE/DEAD Fixable Blue Dead Cell Stain Kit (Life Technologies) or Fixable Viability Stain 510 (BD Biosciences) prior to incubation with extracellular and intracellular Abs, as described above. Immunophenotyping included the identification of surface markers (MHC-II, CD80, CD86, CD206, and CD62L) and cytokines (IFN-γ, TNF-α, IL-10, and TGF-β) expressed by viable $CD11b^+Ly6G^+OVA^-$ or $CD11b^+Ly6G^+OVA^+$ cells and $CD11b^+F4/80^+OVA^-$ or $CD11b^+F4/80^+OVA^+$ cells in the maternal peripheral blood at mid (10.5 dpc) and late (16.5 dpc) pregnancy. The expression of the same cell surface markers and cytokines was evaluated on viable $CD11b^+Ly6G^+OVA^+$ cells and $CD11b^+F4/80^+OVA^+$ cells in the myometrial tissues at mid (10.5 dpc) and late (16.5 dpc) pregnancy. The expression of the MHC class I molecules $H2K^b$ and $H2K^d$ was evaluated on viable $CD11b^+Ly6G^+OVA^+$ and $CD11b^+F4/80^+OVA^+$ cells from the maternal peripheral blood (50 μL) at mid-gestation (10.5 dpc). Data were analyzed with FlowJo software v10.

2.8 | Phagocytosis assays

2.8.1 | Generation of GFP^+ placental particles from mice

To obtain GFP^+ placental particles, DBA/2 female mice were mated with GFP^+ males and the placentas were collected at 17.5 dpc. After collection, the placentas were placed in a Petri dish with PBS and the expression of GFP was determined by *ex vivo* imaging with the IVIS Spectrum in vivo imaging system (PerkinElmer).[85] An excitation filter of 465 nm and an emission filter of 520 nm were used to determine GFP expression. GFP^+ placenta-derived particles were prepared by using a mechanical tissue homogenizer. Whole cells and large cell fragments were removed by centrifugation at 1000 × g for 5 min. Tissue homogenates from one placenta were divided into four aliquots, and GFP^+ placenta-derived particles were collected by centrifugation at 16,000 × g for 5 min. One aliquot of placenta-derived particles was opsonized with 50 μL autologous plasma for 30 min at 37°C and used for phagocytosis assays.

2.8.2 | Phagocytosis of placenta-derived particles or *Escherichia coli* by murine maternal peripheral Ly6G$^+$ and F4/80$^+$ cells

Whole blood samples were collected from pregnant C57BL/6 dams (mated with BALB/c males) at 10.5 dpc or 16.5 dpc (n = 6 each). Whole maternal blood (50 μL) was then incubated with 10 μL of GFP$^+$ placenta-derived particles or 10 μL of pHrodo™ Green *Escherichia coli* (*E. coli*) BioParticles (Life Technologies) for 15 min at 37°C or on ice. After incubation, the cells were washed with FACS stain buffer (BD Biosciences) and centrifuged at 400 × *g* for 5 min. The cells were then incubated with anti-mouse CD11b Alexa Fluor594, anti-mouse F4/80 APC, and anti-mouse Ly6G APC-Cy7 Abs (Supplementary Table S1) in FACS staining buffer (BD Biosciences) for 30 min at 4°C in the dark. After incubation, erythrocytes were lysed by using Ammonium-Chloride-Potassium (ACK) lysing buffer (Lonza, Walkersville, MD), and the resulting leukocytes were collected after centrifugation at 400 × *g* for 5 min. Finally, the cells were washed and resuspended in 500 μL of FACS staining buffer and acquired by using the BD LSRFortessa flow cytometer and FACSDiva 9 software. The analysis was performed and plots were created with FlowJo software v10. The percentage of active phagocytic cells was calculated as the percentage of phagocytic cells at 37°C minus the percentage of phagocytic cells on ice.

2.8.3 | Phagocytosis of cytotrophoblast-derived particles or *Escherichia coli* by human maternal peripheral CD15$^+$ and CD14$^+$ cells

Human peripheral blood samples were collected from healthy pregnant women in the second or third trimester by venipuncture into collection tubes containing EDTA (n = 4 – 6 each). Peripheral blood mononuclear cells (PBMCs) and polymorphonuclear neutrophils (PMNs) were isolated by using Polymorphprep™ (Alere Technologies, Oslo, Norway), following the manufacturer's instructions. After gradient separation, PBMCs and PMNs were washed with 1× PBS (Life Technologies). Cells were resuspended in RPMI 1640 medium (Life Technologies) supplemented with 5% human serum (Sigma–Aldrich) and 1% penicillin/streptomycin antibiotics (Life Technologies) at a concentration of 5 × 10^6 cells/mL. Swan71 human first-trimester cytotrophoblast cells[86] were maintained in Dulbecco's modified Eagle's medium (Life Technologies) supplemented with 10% fetal bovine serum (Life Technologies) and 1% penicillin/streptomycin antibiotics. Swan71 cells were collected and labeled, using Vybrant® DiO cell-labeling solution (Life Technologies), and then 1 × 10^7 DiO-labeled Swan71 cells were homogenized by using a mechanical tissue homogenizer. Whole cells and cell nuclei were removed by centrifugation at 2000 × *g* for 5 min, after which the labeled Swan71-derived particles were collected by centrifugation at 16,000 × *g* for 5 min. The Swan71-derived particles were opsonized with 100 μL human sera for 30 min at 37°C. Then, 5 × 10^5/100 μL of combined PBMCs and PMNs were incubated with 20 μL of Swan71-derived particles or 20 μL of pHrodo™ Green *E. coli* BioParticles for 15 min at either 37°C or on ice. After incubation, the PBMCs and PMNs were washed and centrifuged at 300 × *g* for 5 min followed by incubation with mouse anti-human CD15 BV650 (BD Biosciences) and mouse anti-human CD14 BUV395 (BD Biosciences) Abs in FACS staining buffer for 30 min at 4°C in the dark. Finally, the cells were washed and resuspended in 500 μL of FACS staining buffer and acquired by using a BD LSRFortessa flow cytometer and FACSDiva 9 software. The analysis was performed and plots were created with FlowJo software v10. The percentage of active phagocytic cells was calculated as the percentage of phagocytic cells at 37°C minus the percentage of phagocytic cells on ice.

2.9 | Immunofluorescence and confocal microscopy of in vitro phagocytosis

Murine CD11b$^+$ leukocytes were isolated from whole blood by using CD11b MicroBeads (Miltenyi Biotec, San Diego, CA). Briefly, 300 μL mouse whole blood was lysed with ACK lysing buffer for 5 min on ice to remove erythrocytes. Leukocytes were collected by centrifugation at 400 × *g* for 5 min. CD11b$^+$ cells were selected by isolation using CD11b MicroBeads, according to the manufacturer's instructions. CD11b$^+$ cells were placed into 8-well Lab-Tek chamber slides (Themo Fisher Scientific) with RPMI 1640 medium (Life Technologies). Chamber slides were incubated for 15 min at 37°C. After incubation, 10 μL of GFP$^+$ placental fragments or 10 μL pHrodo™ Green *E. coli* BioParticles were added to RPMI 1640 medium for 30 min at 37°C. Cells were then fixed with 4% paraformaldehyde and immediately used for immunofluorescence staining. Next, slides were blocked by using Antibody Diluent/Block (PerkinElmer, Boston, MA) for 30 min at RT. Slides were then incubated with rat anti-mouse CD11b Alexa Fluor 594, followed by incubation with goat anti-rat IgG Alexa Fluor 594 (Supplementary Table S1). Immunofluorescence signal was visualized with a Zeiss LSM 780 laser scanning confocal microscope as described above. Immunofluorescence signals for Alexa Fluor 647, Alexa Fluor 594, and green fluorescence were excited with a 633 nm HeNe laser, a 550 nm HeNe laser, and a 488 nm line of multiline argon laser, respectively. The DAPI signal was excited with a 405 nm diode laser.

Human PBMCs and PMNs were seeded into a 4-well Lab-Tek chamber slide with RPMI 1640 medium supplemented with 5% human serum and 1% penicillin/streptomycin antibiotics at a concentration of 5 × 10^6 cells/mL. Cells were incubated for 1 h at 37°C to allow for attachment to the chamber slide. Unattached cells were then removed, and new medium was added. Next, 20 μL of Swan71 fragments or 20 μL of pHrodo™ Green *E. coli* BioParticles were added to RPMI 1640 medium for 2 h at 37°C. After incubation, cells were then fixed with 4% paraformaldehyde and washed with 1× PBS. Next, slides were blocked by using Antibody Diluent/Block (PerkinElmer, Boston, MA) for 30 min at RT. Slides were then incubated with mouse anti-human CD14 (BD Biosciences) at RT for 1 h. Following incubation, slides were washed with PBST (1× PBS containing 0.1% Tween 20 [Sigma-Aldrich]) and goat anti-mouse IgG Alexa Fluor 594 (BD Biosciences) was added and incubated for 30 min at RT. Next, slides were incubated with mouse

anti-human CD15 Alexa Fluor 647 (BD Biosciences) for another hour at RT. Finally, slides were washed and mounted with Prolong Gold Antifade Mountant with DAPI. Immunofluorescence signals were visualized with a Zeiss LSM 780 laser scanning confocal microscope as described above.

2.10 | Statistics

Statistical analyses were performed by using SPSS v19.0 (IBM Corporation, Armonk, NY) or GraphPad Prism v8.0.1 for Windows (GraphPad Software, San Diego, CA). The Shapiro-Wilk test was performed to determine the normality of the data. For the proportions of immune cells carrying the fetal Ag throughout pregnancy, the statistical significance between groups was determined by using the Kruskal-Wallis test, followed by Dunn's post-hoc test. The statistical significance between groups for the immunophenotyping at 10.5 dpc and 16.5 dpc as well as the human and murine phagocytosis experiments was determined by using Mann–Whitney *U*-tests. A *P*-value ≤ 0.05 was considered statistically significant.

3 | RESULTS

3.1 | Localization of the fetal Ag to Ly6G$^+$ and F4/80$^+$ cells in the murine myometrium and maternal circulation throughout pregnancy

Fetal Ags are released into the maternal circulation,[44–46] a fraction of which are localized in the reproductive tissues.[87,88] However, whether such Ags are found in tissue-resident innate immune cells is unknown. Herein, we first investigated the presence of the fetal Ag in Ly6G$^+$ and F4/80$^+$ cells residing in the myometrium surrounding the embryo using a model of B6 CAG-OVA males mated with wild type BALB/c females (Fig. 1A). The myometrial tissues surrounding the fetus and placenta were collected at 10.5 dpc, 16.5 dpc, or 18.5 dpc (Fig. 1A). H&E staining provided an anatomical overview to serve as a reference for subsequent immunofluorescence staining (Fig. 1A). Given that CD11b (a cell surface marker for cells of myeloid origin) is expressed by both monocytes and granulocytes,[89–93] we evaluated the intracellular expression of the OVA protein inside CD11b$^+$ cells in the myometrial tissues from 10.5 dpc, 16.5 dpc, and 18.5 dpc. Confocal microscopy revealed localization of the OVA protein inside of myeloid cells in the myometrium, suggesting that local innate immune cells carry the fetal Ag (Fig. 1A). Isotype staining confirmed that the visualization of the OVA protein within such cells was not due to non-specific staining (Fig. S1). To further demonstrate the specificity of the observed OVA signal in myometrial CD11b$^+$ cells, we similarly evaluated the intracellular expression of the OVA protein in dams mated with B6 non-CAG-OVA males (Supplementary Fig. S2). A positive OVA signal was not observed in myometrial CD11b$^+$ cells from dams mated with B6 non-CAG-OVA males when using the anti-OVA Ab (Supplementary Fig. S2A) or isotype control (Supplementary Fig. S2B).

Next, we explored whether fetal Ag-carrying cells could be detected and visualized in the maternal circulation during mid-pregnancy (10.5 dpc). Indeed, Ly6G$^+$OVA$^+$ and F4/80$^+$OVA$^+$ cells were found in peripheral blood samples. Intracellular immunofluorescence staining was utilized to confirm the expression of OVA in sorted innate immune cells from the maternal circulation (Fig. 1B). These findings show that innate immune cells carrying the fetal Ag are present in the myometrium as well as the maternal circulation.

3.2 | The local and systemic proportions of fetal Ag-carrying Ly6G$^+$ and F4/80$^+$ cells change throughout murine pregnancy

Given that the fetal Ag (OVA) was detected in Ly6G$^+$ and F4/80$^+$ cells in the myometrium and maternal circulation, we next investigated whether the proportions of these fetal antigen-carrying cells changed throughout pregnancy. B6 CAG-OVA males were mated with wild type BALB/c (non-CAG-OVA) females, and the myometrial tissues and maternal peripheral blood were collected at 4.5 dpc (early pregnancy; Trypan blue staining was utilized to detect implantation sites), 10.5 dpc (mid-pregnancy), 16.5 dpc (late pregnancy), and 18.5 dpc (term pregnancy) as well as postpartum (PP) (Fig. 2A). The populations of Ly6G$^+$OVA$^+$ and F4/80$^+$OVA$^+$ cells were determined in the myometrium and maternal circulation at each time point. The intracellular expression of OVA by CD4$^+$ and CD8$^+$ T cells was also examined, but these cells did not carry the fetal Ag in the maternal circulation (Supplementary Fig. S3A).

The proportion of myometrial Ly6G$^+$OVA$^+$ cells drastically increased from 4.5 dpc to 10.5 dpc and was largely maintained until term (18.5 dpc), subsequently declining in the PP period (Fig. 2B). The proportion of myometrial F4/80$^+$OVA$^+$ cells peaked at 10.5 dpc and showed a slower decline from this point to PP (Fig. 2C). In the peripheral blood, a large proportion of Ly6G$^+$OVA$^+$ cells was observed at each time point, including PP (Fig. 2D). The proportion of peripheral Ly6G$^+$OVA$^+$ cells followed a similar trajectory to that in the myometrial tissues but with less variation, gradually increasing from 4.5 dpc to 10.5 dpc and then modestly declining in the PP period (Fig. 2D). In contrast, the proportion of F4/80$^+$OVA$^+$ cells in the peripheral blood was lower than that of Ly6G$^+$OVA$^+$ cells at each time point, yet followed an overall similar trend (Fig. 2E). To confirm the presence of OVA$^+$ cells in the myometrium and peripheral blood, we repeated the above experiment using tissues obtained from dams mated with B6 non-CAG-OVA males (Supplementary Fig. S3B). A positive OVA signal was not detected in Ly6G$^+$ or F4/80$^+$ cells in the myometrial tissues (Supplementary Fig. S3C and D) nor in the peripheral blood (Supplementary Fig. S3E and F).

Fetal cells are found in the maternal circulation during pregnancy and persist through the postpartum period; yet, these are rare.[44,45,47] Therefore, we confirmed the maternal origin of phagocytes carrying the OVA Ag in the myometrium and peripheral blood (Fig. 3A and B). Ly6G$^+$OVA$^+$ and F4/80$^+$OVA$^+$ cells in both the myometrium (Fig. 3C) and peripheral blood (Fig. 3D) expressed H2K^d (maternal MHC-I

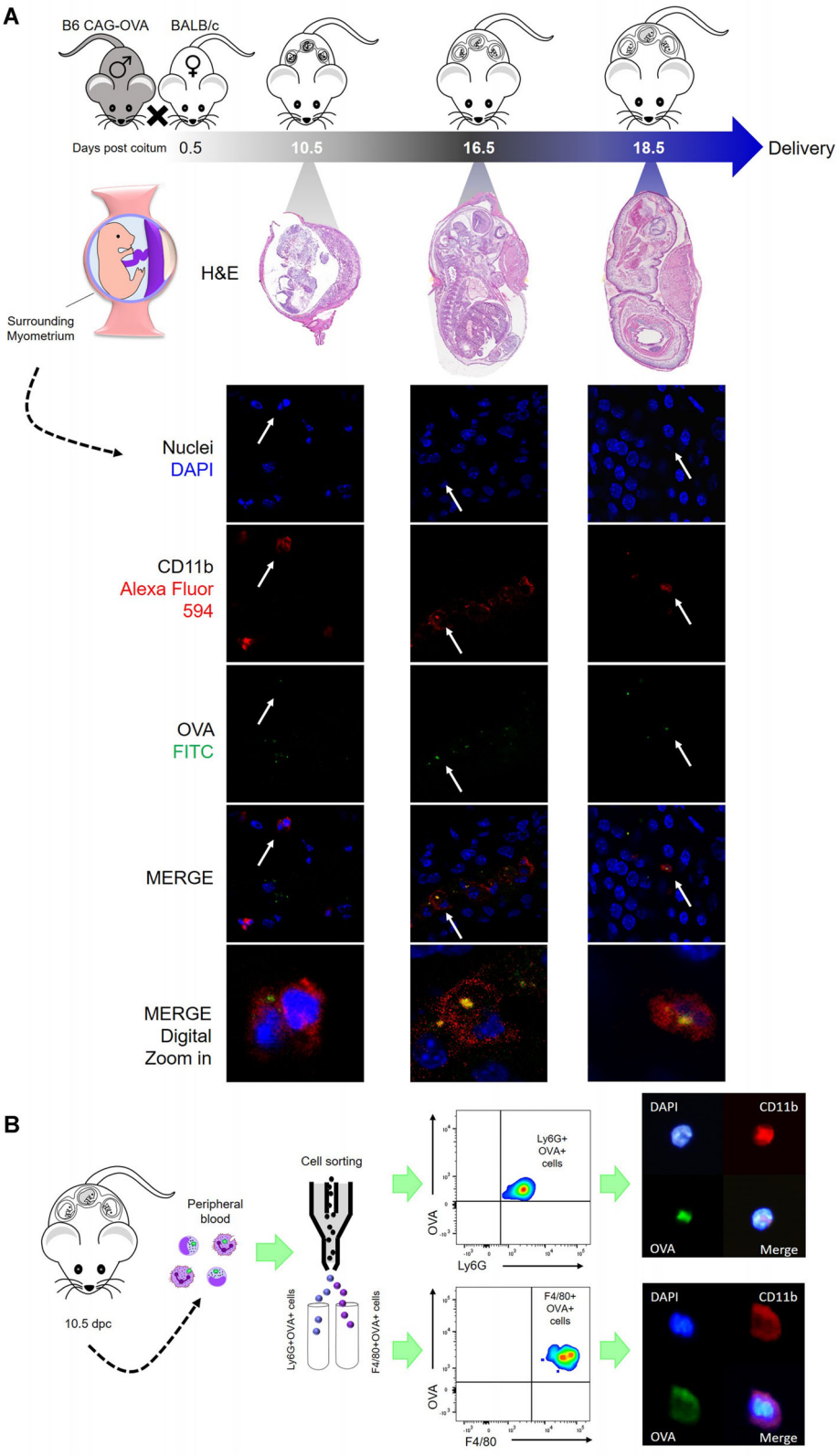

FIGURE 1 **Localization of fetal Ag-carrying Ly6G$^+$ and F4/80$^+$ cells in the murine myometrial tissues and maternal circulation in the second half of pregnancy. (A)** BALB/c females were mated with B6 CAG-OVA males, and the fetuses with surrounding myometrial tissues were collected at 10.5 days *post coitum* (dpc), 16.5 dpc, or 18.5 dpc. Representative images of the fetuses and surrounding myometrial tissues from 10.5 dpc, 16.5 dpc, and 18.5 dpc stained with hematoxylin and eosin (H&E) (4× magnification), and confocal microscopy imaging of DAPI$^+$CD11b$^+$OVA$^+$ cells (indicated by white arrows) in the myometrial tissues (100× magnification with digital zoom) (n = 10 each). **(B)** Fluorescence-activated cell sorting (FACS) of maternal circulating CD11b$^+$Ly6G$^+$OVA$^+$ and CD11b$^+$F4/80$^+$OVA$^+$ cells. Representative fluorescence microscopy images of sorted Ly6G$^+$OVA$^+$ and F4/80$^+$OVA$^+$ cells. Blue = 4′,6-diamidino-2-phenylindole (DAPI), red = CD11b, green = OVA (40× magnification with digital zoom) (n = 10).

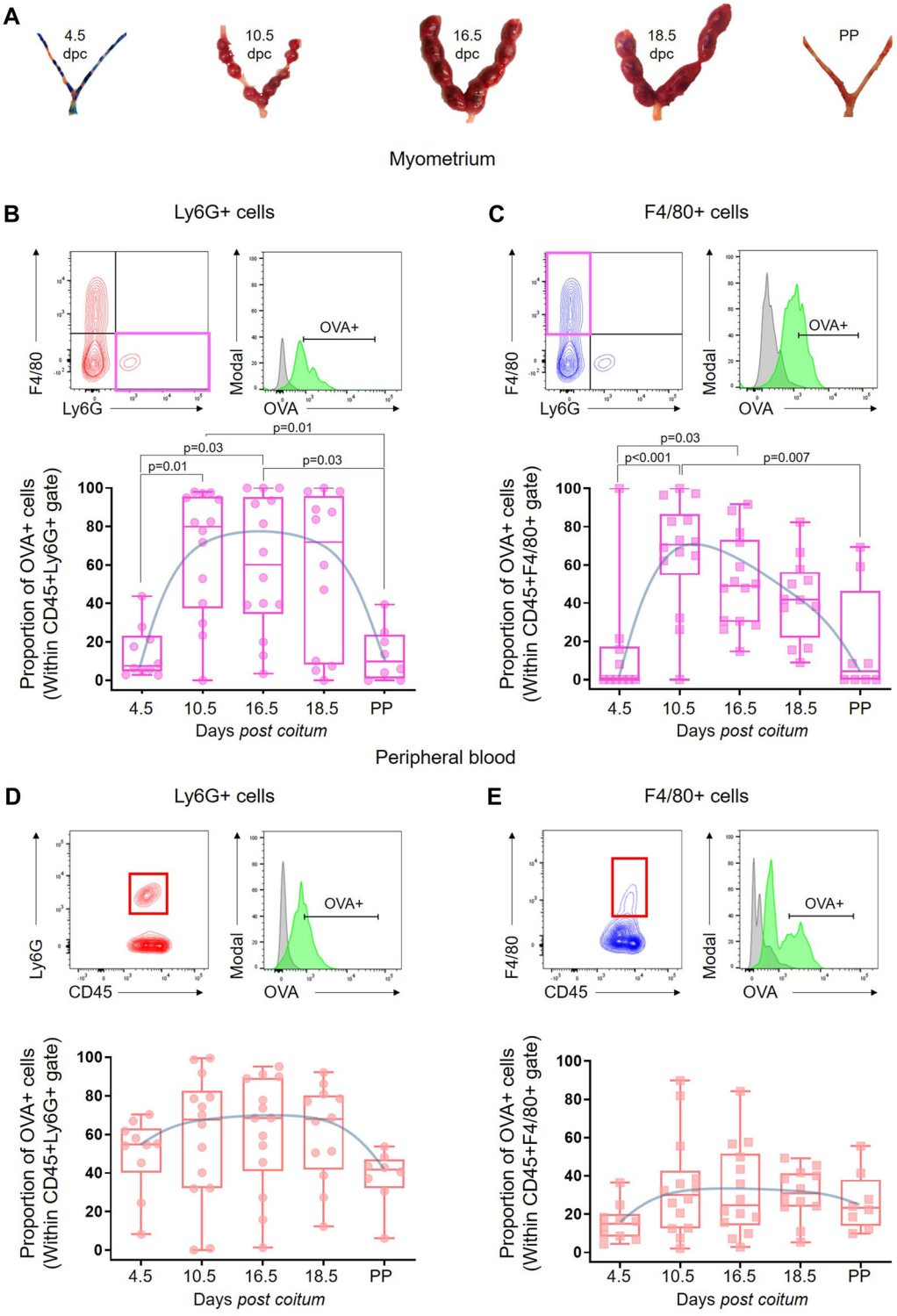

FIGURE 2 **Proportions of fetal Ag-carrying Ly6G$^+$ and F4/80$^+$ cells in the myometrial tissues and the maternal circulation throughout murine pregnancy. (A)** Representative images of the uterine horns from BALB/c females mated with B6 CAG-OVA males at 4.5 days *post coitum* (dpc), 10.5 dpc, 16.5 dpc, or 18.5 dpc and postpartum (PP). **(B and C)** Representative gating strategies and proportions of **(B)** CD45$^+$Ly6G$^+$OVA$^+$ cells and **(C)** CD45$^+$F4/80$^+$OVA$^+$ cells in the myometrial tissues at 4.5 dpc, 10.5 dpc, 16.5. dpc, 18.5 dpc, and PP (n = 8 – 14 each). **(D and E)** Representative gating strategies and proportions of **(D)** CD45$^+$Ly6G$^+$OVA$^+$ cells and **(E)** CD45$^+$F4/80$^+$OVA$^+$ cells in the peripheral blood at 4.5 dpc, 10.5 dpc, 16.5. dpc, 18.5 dpc, and PP (n = 8 – 14 each). Green histogram = anti-OVA; Grey histogram = isotype. Data are shown as box-and-whisker plots where midlines indicate medians, boxes indicate interquartile ranges, and whiskers indicate minimum and maximum ranges. The *P*-values were determined using Kruskal-Wallis tests followed by correction for multiple comparisons. Blue lines indicate changes in the trends for the proportions of Ly6G$^+$OVA$^+$ and F4/80$^+$OVA$^+$ cells throughout pregnancy.

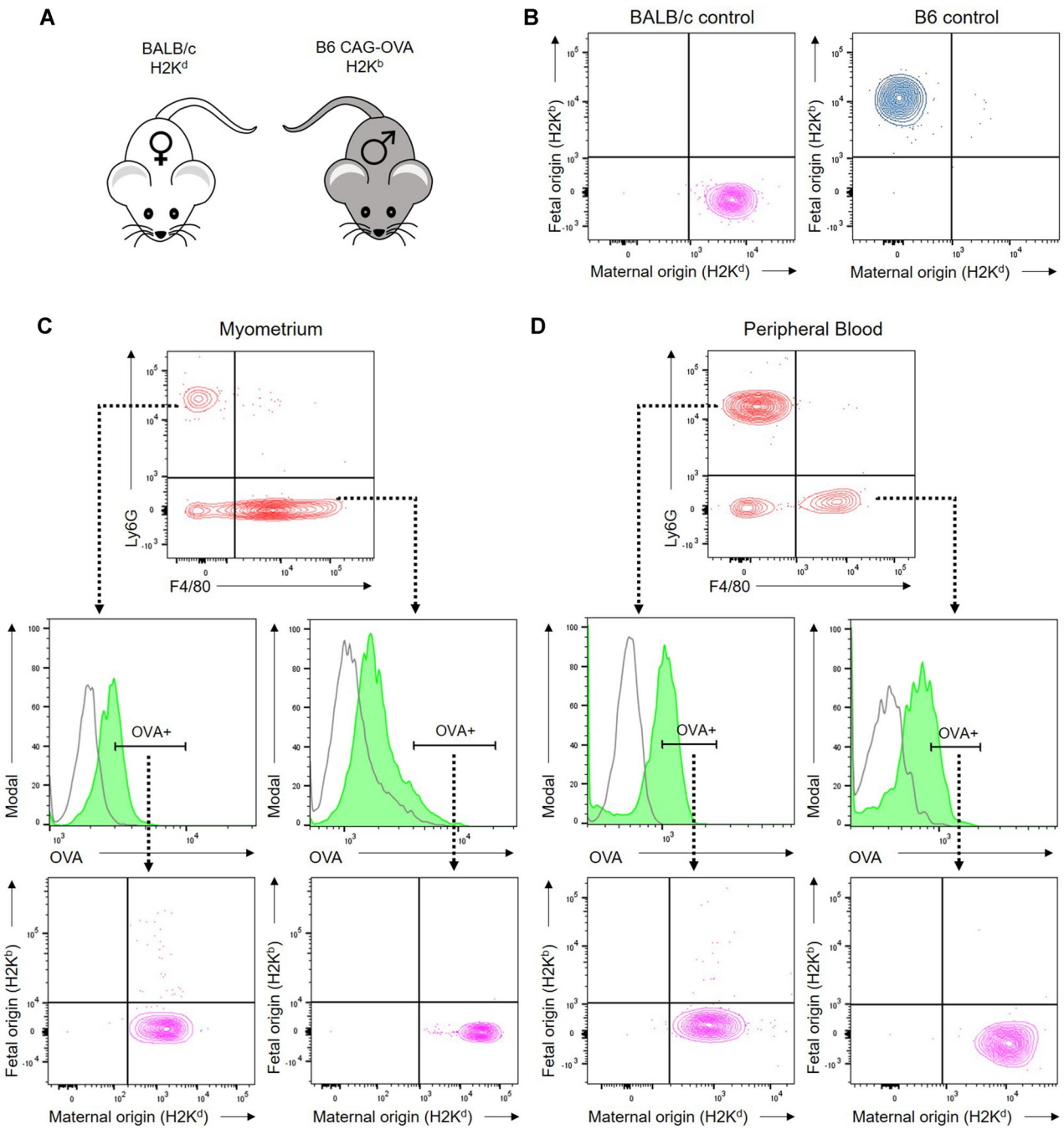

FIGURE 3 Identification of MHC class I ($H2K^d$ or $H2K^b$) to determine the maternal or fetal origin of $Ly6G^+OVA^+$ or $F4/80^+OVA^+$ cells in the murine myometrium and peripheral blood. (A) Representation of haplotypes: BALB/c females display an $H2K^d$ haplotype and B6 CAG-OVA males display an $H2K^b$ haplotype. **(B)** Positive BALB/c controls showing $H2K^d$ expression and B6 controls showing $H2K^b$ expression in the peripheral leukocytes. **(C and D)** Flow cytometry gating strategies and plots showing the expression of $H2K^d$ haplotype and the absence of $H2K^b$ confirming the maternal origin of $Ly6G^+OVA^+$ and $F4/80^+OVA^+$ cells (green histogram = anti-OVA; grey histogram = isotype) in the myometrium and in the maternal circulation (n = 4).

haplotype) and lacked $H2K^b$ (paternal MHC-I haplotype), indicating their maternal origin.

Together, these results indicate that the proportions of fetal Ag-carrying $Ly6G^+$ cells (neutrophils) and $F4/80^+$ cells (monocytes/macrophages) in the myometrium and peripheral blood are highest during the second half of pregnancy and decline after delivery. Hereafter, we primarily focused on investigating the phenotypic and functional properties of such innate immune cells in the maternal circulation to further explore systemic maternal-fetal crosstalk, a poorly understood phenomenon.

3.3 | Fetal Ag-carrying Ly6G$^+$ and F4/80$^+$ cells in the murine maternal circulation display unique phenotypes

We next characterized the phenotypes of fetal antigen-carrying Ly6G$^+$ and F4/80$^+$ cells in the maternal circulation during mid and late pregnancy to determine whether these cells were distinct from their fetal antigen-negative counterparts. Maternal peripheral blood was collected at 10.5 dpc and 16.5 dpc from wild-type BALB/c females mated with B6 CAG-OVA males, and immunophenotyping of Ly6G$^+$OVA$^+$ or Ly6G$^+$OVA$^-$ cells and F4/80$^+$OVA$^+$ or F4/80$^+$OVA$^-$ cells was performed (Fig. 4A). We first examined the expression of MHC-II, an essential molecule for Ag presentation by Antigen-Presenting Cells (APCs),[94] and found that the expression of MHC-II was significantly higher on Ly6G$^+$OVA$^+$ cells compared to Ly6G$^+$OVA$^-$ cells at 10.5 dpc and tended to increase at 16.5 dpc (Fig. 4B). A similar trend was observed for the expression of MHC-II by F4/80$^+$OVA$^+$ cells, although this did not reach statistical significance (Fig. 4C). We also investigated the expression of the co-stimulatory molecules CD80 and CD86[95] by OVA$^+$ and OVA$^-$ innate immune cells. The expression of CD80 by Ly6G$^+$OVA$^+$ cells was elevated in the peripheral blood compared to Ly6G$^+$OVA$^-$ cells at both 10.5 dpc and 16.5 dpc (Fig. 4D). However, the expression of CD80 by F4/80$^+$OVA$^+$ cells was similar to that of F4/80$^+$OVA$^-$ cells (Fig. 4E). Although the expression of CD86 by Ly6G$^+$OVA$^+$ cells did not differ from that of Ly6G$^+$OVA$^-$ cells (Fig. 4F), the expression of this co-stimulatory molecule was increased by F4/80$^+$OVA$^+$ cells compared to F4/80$^+$OVA$^-$ cells at 10.5 dpc and 16.5 dpc (Fig. 4G). No significant differences were observed in the expression of the activation markers CD206[96–99] and CD62L[100–103] by OVA$^+$ and OVA$^-$ innate immune cells (Fig. 4H-K).

We also performed immunophenotyping of myometrial Ly6G$^+$OVA$^+$ and F4/80$^+$OVA$^+$ cells to measure the expression of the molecules that were determined in OVA$^+$ innate immune cells in the maternal circulation (Supplementary Fig. S4A). Comparative analysis between OVA$^+$ and OVA$^-$ immune cells in the myometrial tissues was not possible since very few OVA$^-$ leukocytes were found in these tissues. Therefore, we report differences between 10.5 dpc and 16.5 dpc. We found that the phenotypes of OVA$^+$ myometrial innate immune cells differed between 10.5 dpc and 16.5 dpc (Figure S4B-K).

Together, these data show that fetal Ag-carrying Ly6G$^+$ cells (i.e., neutrophils) and F4/80$^+$ cells (i.e., monocytes) display unique phenotypes in the maternal circulation.

3.4 | Fetal Ag-carrying Ly6G$^+$ and F4/80$^+$ cells display a homeostatic cytokine profile in the murine maternal circulation

Next, we investigated the expression of pro-inflammatory (IFN-γ and TNF-α) and anti-inflammatory (IL-10 and TGF-β) cytokines by Ly6G$^+$OVA$^+$ or Ly6G$^+$OVA$^-$ cells and F4/80$^+$OVA$^+$ or F4/80$^+$OVA$^-$ cells. Maternal peripheral blood was collected at 10.5 dpc or 16.5 dpc from wild type BALB/c females mated with B6 CAG-OVA males, and immunophenotyping of OVA$^+$ and OVA$^-$ neutrophils and monocytes was performed (Fig. 5A). The expression of IFN-γ by Ly6G$^+$OVA$^+$ cells was significantly decreased compared to that of Ly6G$^+$OVA$^-$ cells at 10.5 dpc and 16.5 dpc (Fig. 5B). Similarly, the expression of TNF-α by Ly6G$^+$OVA$^+$ cells was reduced compared to that of Ly6G$^+$OVA$^-$ cells at 10.5 dpc and 16.5 dpc; yet, significance was only reached at 10.5 dpc (Fig. 5C). No significant differences in the expression of IL-10 and TGF-β were observed between Ly6G$^+$OVA$^+$ and Ly6G$^+$OVA$^-$ cells (Fig. 5D and E). Although the expression of IFN-γ and TNF-α was similar between F4/80$^+$OVA$^+$ and F4/80$^+$OVA$^-$ cells (Fig. 5F and G), the expression of IL-10 by F4/80$^+$OVA$^+$ cells was greater than that of F4/80$^+$OVA$^-$ cells at 10.5 dpc and 16.5 dpc; yet, significance was only reached at 16.5 dpc (Fig. 5H). Interestingly, the expression of TGF-β by F4/80$^+$OVA$^+$ cells was greater than that of F4/80$^+$OVA$^-$ cells at both 10.5 dpc and 16.5 dpc (Fig. 5I).

We also performed immunophenotyping of myometrial Ly6G$^+$OVA$^+$ and F4/80$^+$OVA$^+$ cells to measure the expression of cytokines that were determined in OVA$^+$ immune cells in the peripheral blood (Supplementary Fig. S4A). We report that cytokine expression by OVA$^+$ myometrial innate immune cells partially differed between 10.5 dpc and 16.5 dpc (Supplementary Fig. S4L-S).

Collectively, these results suggest that fetal Ag-carrying Ly6G$^+$ cells (i.e., neutrophils) and F4/80$^+$ cells (i.e., monocytes) exhibit homeostatic functions in the maternal circulation by expressing low levels of pro-inflammatory cytokines or increased levels of anti-inflammatory cytokines, respectively.

3.5 | Maternal circulating Ly6G$^+$ and F4/80$^+$ cells phagocytose placenta-derived particles in mid and late murine pregnancy

Up to this point, our results suggest that maternal innate immune cells capture the fetal Ag present in the maternal circulation. Therefore, we next investigated whether particles derived from GFP$^+$ placentas of allogeneic pregnancies were phagocytosed by maternal peripheral Ly6G$^+$ cells and F4/80$^+$ cells from wild type BALB/c dams mated with B6 CAG-OVA males (Fig. 6A). Flow cytometry was utilized to determine the phagocytosis of GFP$^+$ placental particles (Fig. 6B). Both maternal Ly6G$^+$ and F4/80$^+$ cells were capable of phagocytosing placenta-derived particles at 10.5 dpc and 16.5 dpc (Fig. 6C and D). Consistent with the similar proportions of Ly6G$^+$OVA$^+$ and F4/80$^+$OVA$^+$ cells observed between 10.5 dpc and 16.5 dpc, the proportion of phagocytosis did not differ between these gestational time points for either cell type (Fig. 6C and D). As expected, Ly6G$^+$ and F4/80$^+$ cells phagocytosed *E. coli* efficiently, which served as a positive control for phagocytosis, while no differences were observed between 10.5 dpc and 16.5 dpc (Supplementary Fig. S5A-D). Immunofluorescence illustrated the uptake of placenta-derived particles by maternal peripheral myeloid cells (CD11b$^+$ cells; Fig. 6E). Together, these data offer functional evidence that maternal circulating Ly6G$^+$ cells (i.e., neutrophils) and

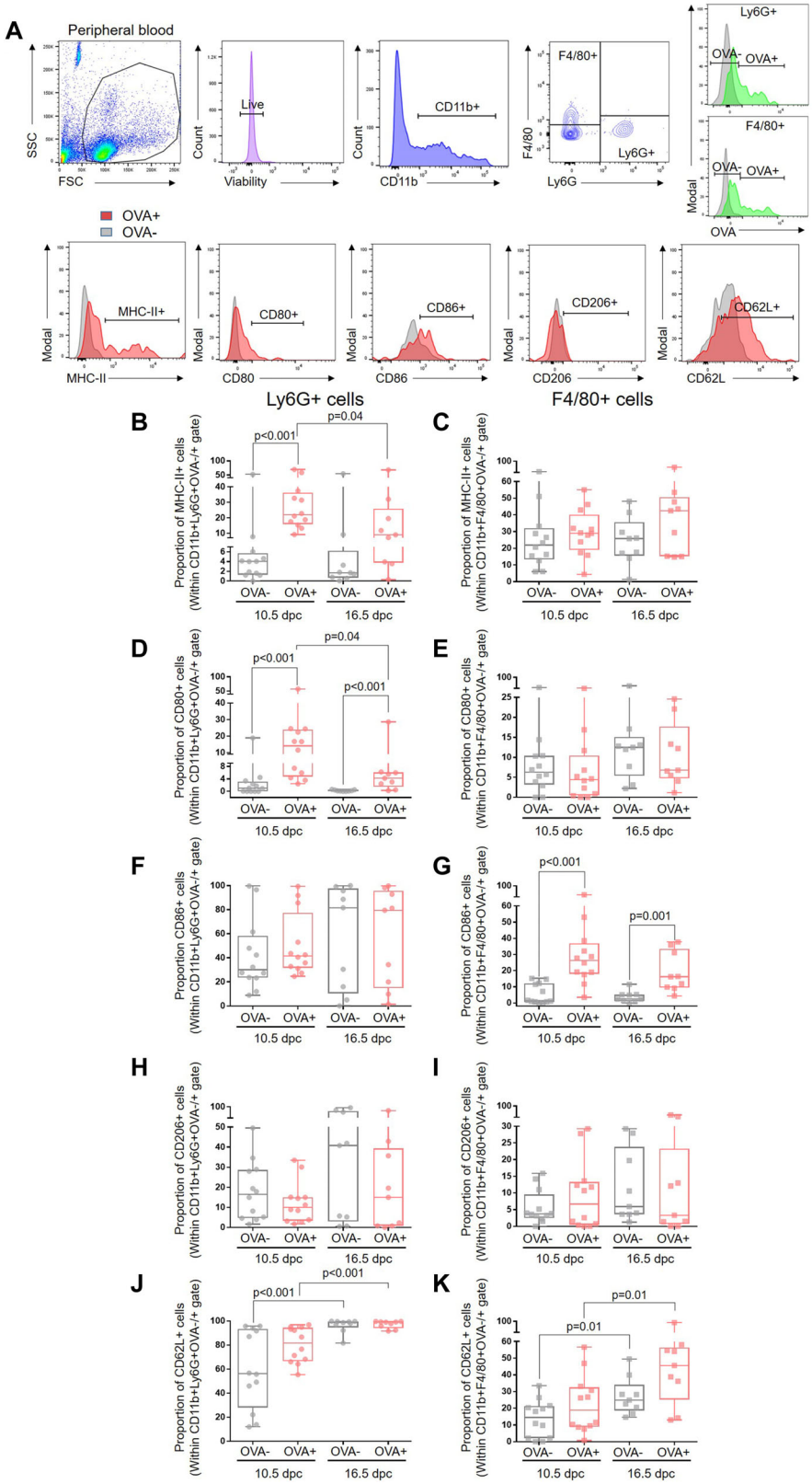

FIGURE 4 **Immunophenotyping of fetal Ag-carrying Ly6G$^+$ and F4/80$^+$ cells in the peripheral blood during mid and late murine gestation.** **(A)** Flow cytometry gating strategy used to determine the Ly6G$^+$OVA$^+$ and F4/80$^+$OVA$^+$ cells or Ly6G$^+$OVA$^-$ and F4/80$^+$OVA$^-$ cells (green histogram = anti-OVA; grey histogram = isotype) in the peripheral blood. Grey or red histograms are shown when referring to OVA$^-$ cells or OVA$^+$ cells, respectively. Proportions of CD11b$^+$Ly6G$^+$OVA$^-$ or CD11b$^+$Ly6G$^+$OVA$^+$ cells and proportions of CD11b$^+$F4/80$^+$OVA$^-$ or CD11b$^+$F4/80$^+$OVA$^+$ cells expressing **(B and C)** MHC-II, **(D and E)** CD80, **(F and G)** CD86, **(H and I)** CD206, or **(J and K)** CD62L in the peripheral blood at 10.5 days *post coitum* (dpc) and 16.5 dpc (n = 9 – 12 each). Grey or red box-plots are shown when referring to OVA$^-$ cells or OVA$^+$ cells, respectively. Data are shown as box-and-whisker plots where midlines indicate medians, boxes indicate interquartile ranges, and whiskers indicate minimum and maximum ranges. The *P*-values were determined using Mann-Whitney *U*-tests.

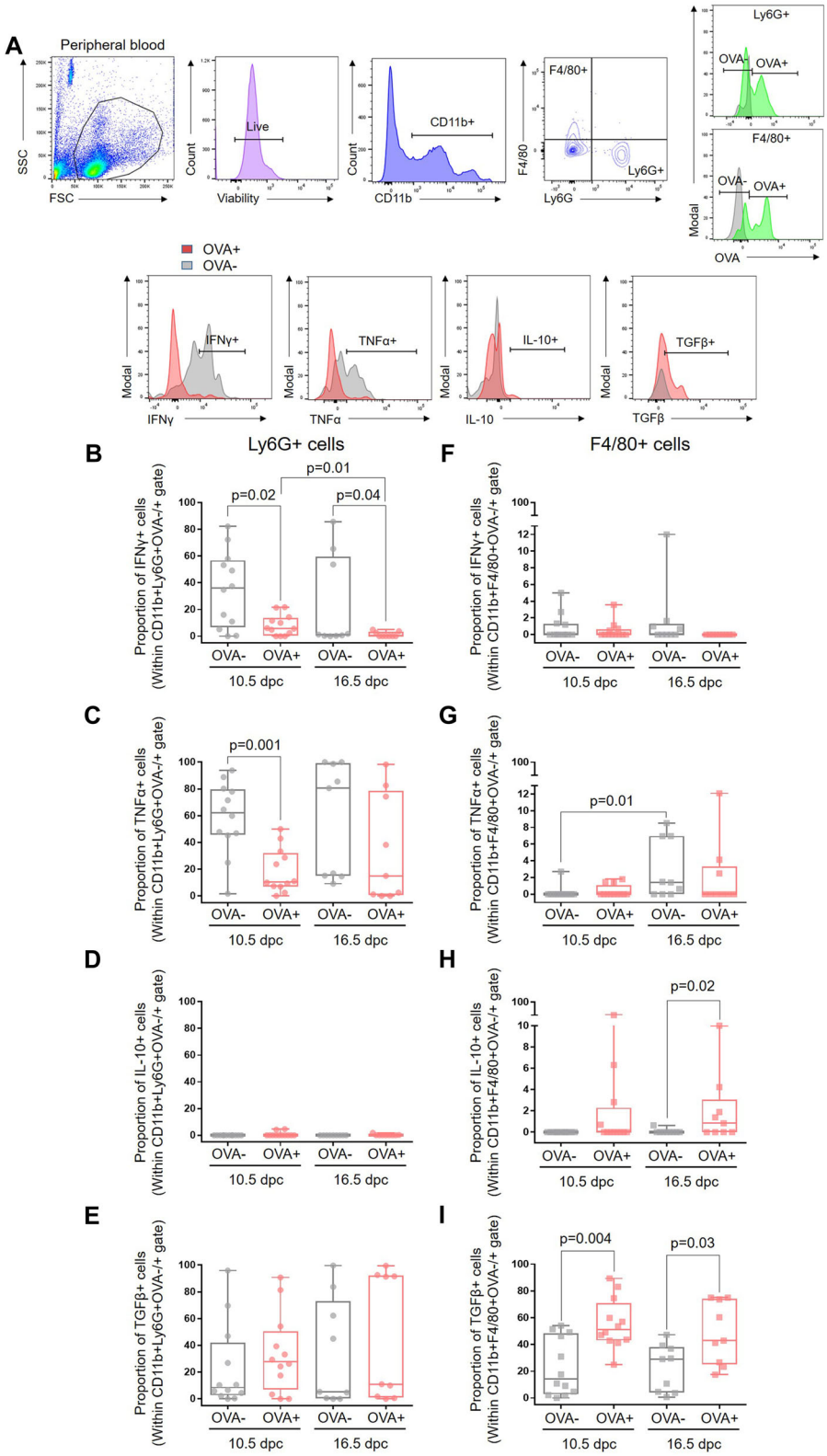

FIGURE 5 **Cytokine expression by fetal Ag-carrying Ly6G$^+$ and F4/80$^+$ cells in the maternal circulation during mid and late murine pregnancy. (A)** Flow cytometry gating strategy used to determine the Ly6G$^+$OVA$^-$ and F4/80$^+$OVA$^-$ cells or Ly6G$^+$OVA$^+$ and F4/80$^+$OVA$^+$ cells (green histogram = anti-OVA; grey histogram = isotype) in the peripheral blood. Grey or red histograms are shown when referring to OVA$^-$ cells or OVA$^+$ cells, respectively. Proportions of CD11b$^+$Ly6G$^+$OVA$^-$ or CD11b$^+$Ly6G$^+$OVA$^+$ cells and proportions of CD11b$^+$F4/80$^+$OVA$^-$ or CD11b$^+$F4/80$^+$OVA$^+$ cells expressing **(B and F)** IFN-γ, **(C and G)** TNF-α, **(D & H)** IL-10, or **(E and I)** TGF-β in the peripheral blood at 10.5 days *post coitum* (dpc) and 16.5 dpc (n = 9 – 12 each). Grey or red box-plots are shown when referring to OVA$^-$ cells or OVA$^+$ cells, respectively. Data are shown as box-and-whisker plots where midlines indicate medians, boxes indicate interquartile ranges, and whiskers indicate minimum and maximum ranges. The *P*-values were determined using Mann-Whitney *U*-tests.

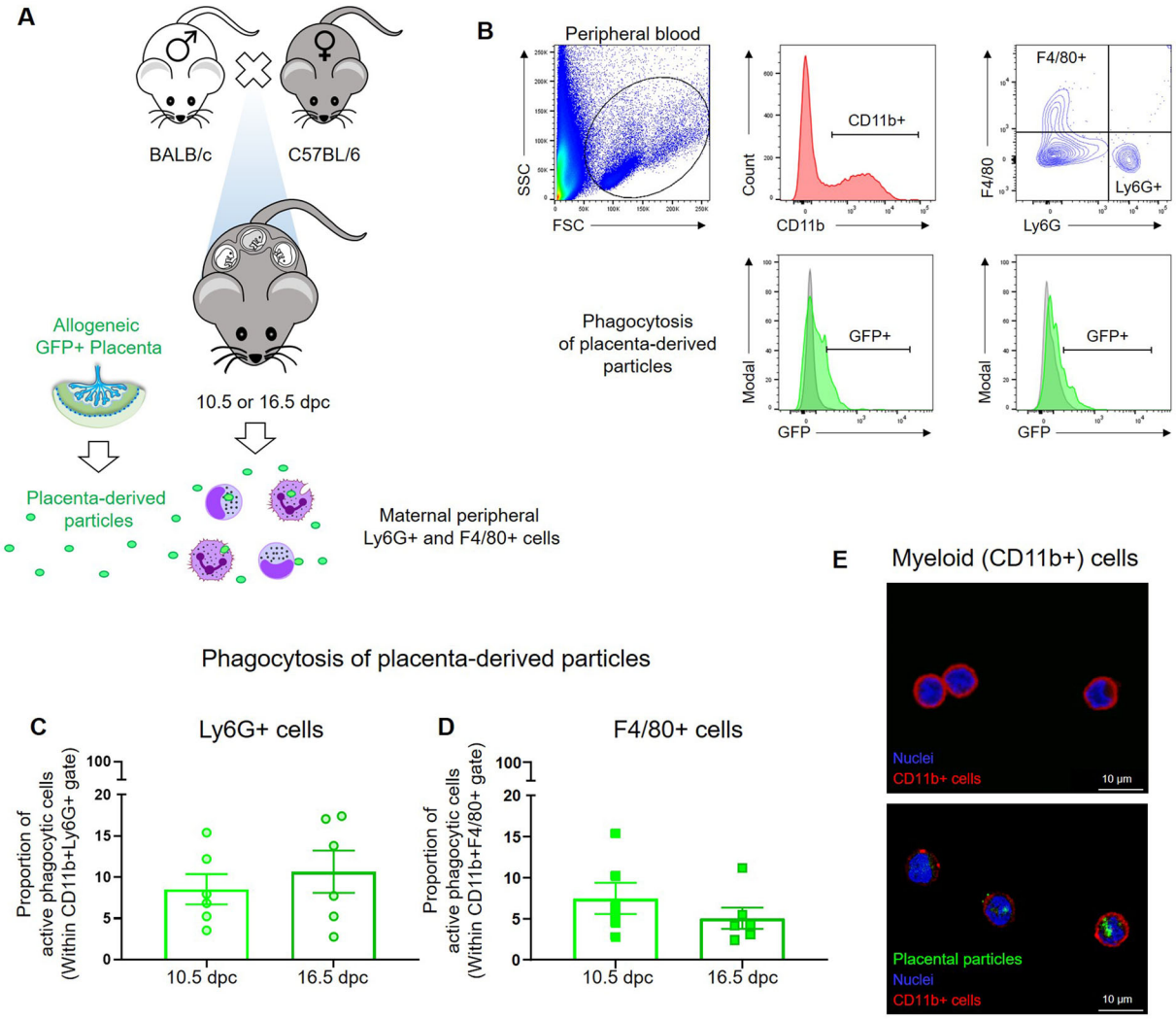

FIGURE 6 **Phagocytosis of placenta-derived particles by maternal Ly6G$^+$ and F4/80$^+$ cells in mid and late murine pregnancy. (A)** Maternal peripheral Ly6G$^+$ cells and F4/80$^+$ cells were collected from wild-type C57BL/6 dams mated with BALB/c males at 10.5 days *post coitum* (dpc) or 16.5 dpc and cultured with placenta-derived particles from a GFP$^+$ allogeneically mated dam (n = 6 each). The uptake of placenta-derived particles by Ly6G$^+$ and F4/80$^+$ cells was evaluated by flow cytometry. **(B)** Representative gating strategy showing the uptake of GFP$^+$ placenta-derived particles by maternal peripheral Ly6G$^+$ and F4/80$^+$ cells. **(C and D)** Proportions of active Ly6G$^+$ cells and F4/80$^+$ cells that phagocytosed GFP$^+$ placenta-derived particles at 10.5 dpc or 16.5 dpc. Data are shown as scatter dot plots where bars indicate the mean and whiskers indicate the standard error of the mean. *P*-values were determined using Mann-Whitney *U*-tests. **(E)** Representative confocal microscopy images showing maternal peripheral myeloid cells (CD11b$^+$ cells) alone (top image) or after phagocytosing GFP$^+$ placenta-derived particles (bottom image). Blue indicates DAPI (nuclei), red indicates CD11b$^+$ cells, and green indicates placenta-derived particles. Scale bars represent 10 μm.

F4/80$^+$ cells (i.e., monocytes) can phagocytose placenta-derived particles during mid and late murine gestation.

3.6 | Maternal circulating CD15$^+$ cells and CD14$^+$ cells phagocytose cytotrophoblast-derived particles in human pregnancy

Lastly, to demonstrate the translational value of our findings in mice, we performed in vitro studies using maternal peripheral CD15$^+$ (i.e., neutrophils) and CD14$^+$ (i.e., monocytes) cells from second- and third-trimester pregnancies to explore whether cytotrophoblast-derived particles can also be engulfed by such innate immune cells (Fig. 7A). Particles were derived from Swan71 cytotrophoblast cells, which have been conventionally utilized for the generation of exosomes for research into maternal-fetal crosstalk.[61,104,105] Flow cytometry was utilized to determine the phagocytosis of DiO-labeled cytotrophoblast-derived particles (Fig. 7B). Consistent with our findings in mice, maternal CD15$^+$ and CD14$^+$ cells phagocytosed cytotrophoblast-derived particles during the second and third trimester (Fig. 7C and D). Such phagocytic activity appeared to be greater in the third trimester compared to the second trimester, but this increase did not reach statistical significance (Fig. 7C and D). Immunofluorescence imaging further demonstrated the uptake of

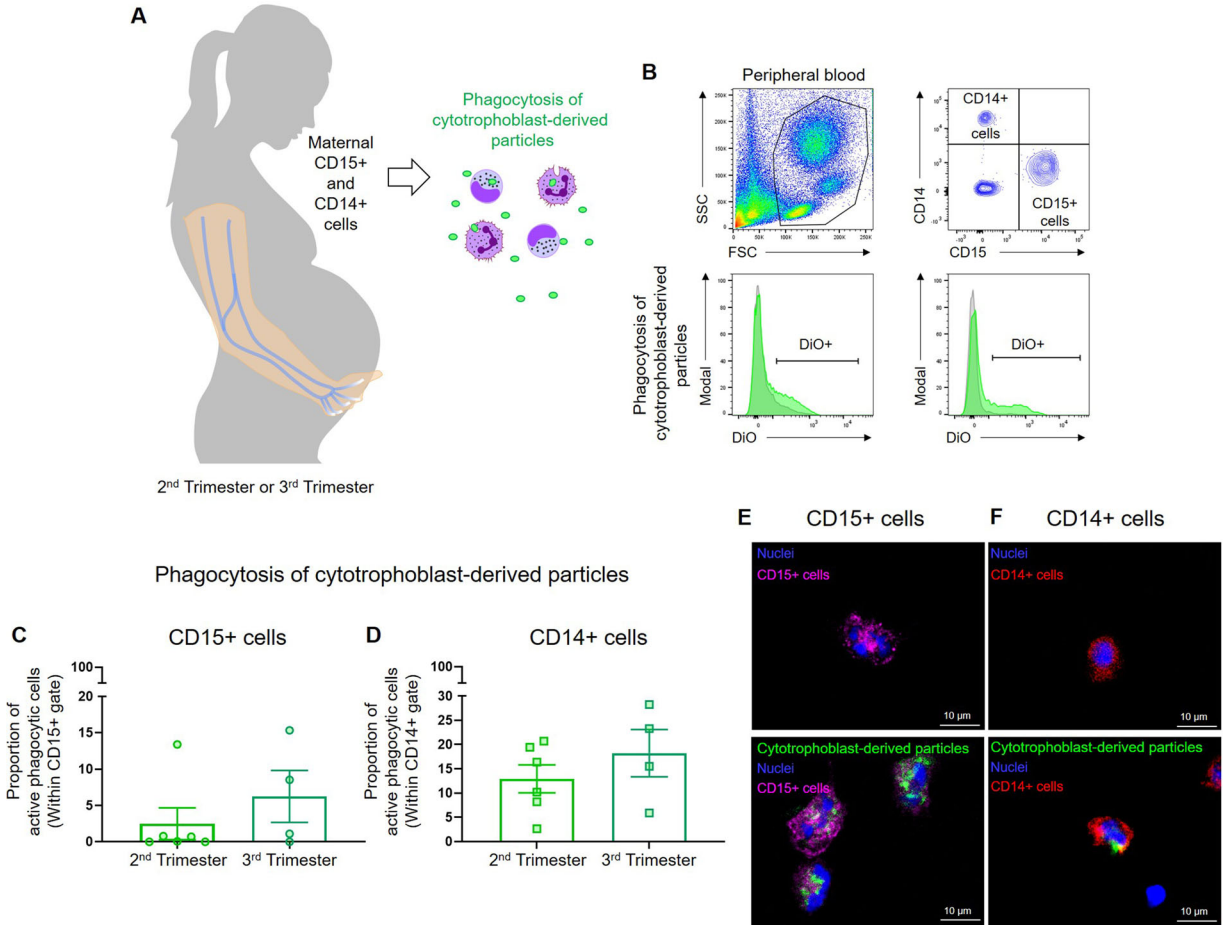

FIGURE 7 Phagocytosis of cytotrophoblast-derived particles by maternal CD15$^+$ neutrophils and CD14$^+$ monocytes in the second and third trimester of human pregnancy. (A) Maternal peripheral CD15$^+$ neutrophils and CD14$^+$ monocytes were collected from pregnant women in the second or third trimester and cultured with particles derived from DiO-labeled cytotrophoblast cells (n = 4 – 6 each). The uptake of cytotrophoblast-derived particles by CD15$^+$ neutrophils and CD14$^+$ monocytes was evaluated by flow cytometry. **(B)** Representative gating strategy showing the uptake of cytotrophoblast-derived particles by maternal peripheral CD15$^+$ neutrophils and CD14$^+$ monocytes. **(C and D)** Proportions of active CD15$^+$ neutrophils and CD14$^+$ monocytes that phagocytosed cytotrophoblast-derived particles in the second or third trimester. Data are shown as scatter dot plots where bars indicate the mean and whiskers indicate the standard error of the mean. *P*-values were determined using Mann-Whitney *U*-tests. **(E)** Representative confocal microscopy images showing maternal peripheral CD15$^+$ neutrophils alone (upper image) or after phagocytosing particles derived from DiO-labeled cytotrophoblasts (bottom image). **(F)** Representative confocal microscopy images showing maternal peripheral CD14$^+$ monocytes alone (upper image) or after phagocytosing particles derived from DiO-labeled cytotrophoblasts (bottom image). Blue immunofluorescence indicates DAPI (nuclei), pink indicates CD15$^+$ cells, red indicates CD14$^+$ cells, and green indicates cytotrophoblast-derived particles. Scale bars represent 10 μm.

cytotrophoblast-derived particles by maternal phagocytes (Fig. 7E and F). As expected, maternal CD15$^+$ cells and CD14$^+$ cells also efficiently phagocytosed *E. coli* (Supplementary Fig. S5E-I). These findings provide translational value to our observations in mice by demonstrating that maternal CD15$^+$ cells (neutrophils) and CD14$^+$ cells (monocytes) are capable of capturing fetus-derived Ags in the maternal circulation during the second and third trimesters.

4 | DISCUSSION

The immune mechanisms implicated in maternal-fetal crosstalk have been extensively investigated in the uterine decidua, given that this is the primary site of interaction between the mother and the developing fetus.[1–3,5] Another established site of maternal-fetal interaction is the intervillous space, which has primarily been studied in the context of in utero transmission of pathogens[106–110] and trans-placental transfer of Abs.[111–115] Fetal Ags can also be found in the maternal circulation,[17,44,45,116–119] where their concentrations increase as gestation progresses[46,85,120–124]; however, their fate is largely unknown. Herein, we provide evidence that fetal Ags can be encountered by neutrophils and monocytes in the maternal circulation.

Neutrophils are the dominant immune cell type in the circulation and therefore play a central role in host responses in both humans and mice. Pregnant women display greater numbers of neutrophils in the

circulation compared to non-pregnant women,[125–128] a phenomenon that is also observed in mice.[129,130] Yet, neutrophil numbers also vary throughout gestation.[125] A recent high-dimensional study confirmed the cellular dynamics of circulating neutrophils during normal gestation and provided evidence of the responsiveness of these innate immune cells to a variety of stimuli.[131] Indeed, neutrophils from pregnant women possess a distinct phenotype from that of non-pregnant women, which is characterized by the enhanced expression of activation markers such as CD14 and CD64.[69,70] Importantly, neutrophil responsiveness toward chemotactic agents (i.e., evidence of leukocyte activation), including those derived from reproductive tissues, is increased as gestation progresses and may serve as a biomarker for pregnancy complications.[71,132–135] Consistently, neutrophil effector functions such as ROS production[69,70,72] and neutrophil extracellular trap (NET) formation[136] are boosted in pregnancy compared to the non-pregnant state. Regarding phagocytosis, one of the main functions of neutrophils, conflicting reports have suggested that this capability may be diminished or improved in pregnancy.[74–76] In the current study, we discovered that maternal neutrophils can phagocytose fetal Ags derived from the placenta throughout gestation. To our knowledge, this is the first demonstration that such a process occurs in the maternal circulation, providing evidence that neutrophils participate in systemic maternal-fetal crosstalk.

Fetal Ag-carrying neutrophils displayed a unique phenotype characterized by the up-regulation of MHC-II and CD80, suggesting that these maternal innate immune cells exhibit APC-like functions. Previous reports have shown that non-pregnant adult neutrophils are capable of Ag presentation, given their ability to phagocytose Ags and express APC markers such as MHC-II, CD80, and CD86.[137–139] However, dendritic cells and monocytes are superior to neutrophils in their capacity for Ag presentation.[140] Our study also demonstrated decreased expression of the pro-inflammatory cytokines IFN-γ and TNF-α by fetal Ag-carrying neutrophils in the maternal circulation. These data imply that, during pregnancy, circulating neutrophils exhibit anti-inflammatory functions, a phenotype that has been termed "N2."[141–143] These results are in tandem with a previous report showing that neutrophils can exhibit homeostatic functions during mid pregnancy.[144] Yet, additional research is required to explore the contribution of neutrophils to fetal Ag presentation and tolerogenic processes in the maternal circulation.

Monocytes represent the primary subset of circulating mononuclear cells and carry out two essential functions: (i) to act as sentinels in the blood vessels, and (ii) to transmigrate across the vessel endothelium to respond to tissue-derived signals or threats.[145] Several reports have indicated that, similar to neutrophils, circulating monocyte numbers increase throughout pregnancy,[78,126,127,146] although this is not consistently observed.[77] Peripheral monocytes display a gradually enhanced state of activation as gestation progresses,[77,147] indicated by elevated cytokine responses[56,79] and phosphorylation of key signaling molecules (e.g., NF-κB).[147] Moreover, pregnancy-derived circulating monocytes display up-regulated expression of multiple activation markers such as CD11b, CD14, and CD64.[69,70,77,78] Indeed, we have recently reported that single-cell RNA sequencing-derived signatures from monocytes and macrophages are modulated in the maternal circulation throughout gestation, and such signatures are increased in women who underwent preterm labor and birth, providing a potential non-invasive biomarker for the pathological process of labor.[148] Consistent with studies of peripheral neutrophils, pregnancy has been separately reported to be associated with decreased or enhanced phagocytic function by circulating monocytes.[75,80] Herein, we observed that peripheral monocytes are capable of engulfing placenta-derived Ags, establishing a potential mechanism whereby these innate immune cells can participate in systemic maternal-fetal interactions.

Fetal Ag-carrying monocytes exhibited a homeostatic phenotype characterized by the up-regulation of CD86 together with an increased expression of TGF-β and IL-10. These findings are consistent with previous reports showing that monocytes/macrophages exhibit immunoregulatory functions during pregnancy.[30,149,150] Specifically, uterine macrophage populations display an alternatively activated phenotype and are involved in embryo implantation and placental development as well as in host defense.[33–35,151–154] Yet, monocytes in the maternal circulation are less characterized, and we are currently engaged in the investigation of their role during the second half of pregnancy. The systemic depletion of monocytes/macrophages induces preterm labor and birth, highlighting the homeostatic functions of these cells during pregnancy.[155] Consistently, the adoptive transfer of M2-polarized (i.e., homeostatic) macrophages prevents preterm birth in animal models of intra-amniotic inflammation.[155–157] Collectively, these data suggest that maternal peripheral monocytes display homeostatic functions during pregnancy, which include the uptake of fetal Ags released by the placenta.

It is worth mentioning that fetal Ag-carrying neutrophils and monocytes were also detected in the postpartum period (i.e., 48-60 h after delivery), and such cells may continue to decline as time progresses. Yet, the presence of these cells may also contribute to immunological memory.[25,26,158–160]

A central question derived from our study concerns the events initiated in maternal neutrophils and monocytes upon fetal Ag uptake. One possibility is that maternal circulating innate immune cells phagocytose the fetal Ag for containment to prevent aberrant Ag-specific T-cell responses that could jeopardize pregnancy homeostasis. Another possibility is that maternal neutrophils and monocytes internalize the fetal Ag for processing and transport to the uterine-draining lymph nodes to be presented by professional APCs, as has been previously proposed,[145,161–163] where indirect Ag presentation occurs.[81] A third possibility is that the fetal Ag is processed and presented by maternal neutrophils and monocytes to either circulating T cells or those in the lymphatic or decidual tissues. However, each of the above hypotheses require mechanistic investigation to ascertain the fate of the fetal Ag in the maternal circulation and how this process contributes to the mechanisms of maternal-fetal tolerance.

The current study has some limitations. The sole use of the F4/80 or CD14 markers does not allow us to distinguish between monocytes and macrophages; yet, it can be reasonably presumed that the majority of circulating maternal OVA$^+$ cells represent monocytes, whereas those in the myometrium are primarily tissue-resident macrophages.

In addition, the characterization of the placenta-derived particles used in the current study, as well as the mechanisms whereby these particles are engulfed by maternal phagocytes, warrants further investigation in future studies. Furthermore, functional characterization of those maternal innate immune cells that are capable of engulfing fetal Ags is required. Lastly, we did not evaluate whether B cells can participate in the uptake of fetal Ags in the maternal circulation because our study was focused on innate immune cells.

In summary, herein we provide evidence that specific maternal innate immune cells are capable of fetal Ag uptake and that such cells are most prevalent in the second half of murine pregnancy. These innate immune cells displayed unique phenotypes: while neutrophils expressed high levels of MHC-II and CD80 together with low levels of pro-inflammatory cytokines, monocytes upregulated the expression of CD86 as well as the anti-inflammatory cytokines IL-10 and TGF-β. Importantly, fetal Ag uptake was also displayed by neutrophils and monocytes from pregnant women, providing translational evidence that this process also occurs in humans. Collectively, these findings demonstrate novel interactions between specific maternal circulating innate immune cells and fetal Ags, thereby shedding light on the peripheral mechanisms of maternal-fetal crosstalk.

ACKNOWLEDGMENTS

This research was supported by the Wayne State University Perinatal Initiative in Maternal, Perinatal and Child Health. This research was also supported, in part, by the Perinatology Research Branch, Division of Obstetrics and Maternal-Fetal Medicine, Division of Intramural Research, *Eunice Kennedy Shriver* National Institute of Child Health and Human Development, National Institutes of Health, U.S. Department of Health and Human Services (NICHD/NIH/DHHS); and, in part, with Federal funds from NICHD/NIH/DHHS under Contract No. HHSN275201300006C. The authors would like to thank Chengrui Zou and Gregorio Martinez III for their assistance in carrying out some of the immunophenotyping and imaging experiments. Dr. Romero has contributed to this work as part of his official duties as an employee of the United States Federal Government.

AUTHORSHIP

M.A.-H. was associated with investigation - experimental performance, data analysis, writing – original draft, writing – review, editing, and revision. R.R. was associated with investigation - study design & data interpretation, writing – review, editing, and revision. M.G. was associated with investigation - experimental performance & data interpretation, writing – original draft, writing – review, editing, and revision. L.T., Y.X., V.G-F., E.P., G.S., and R.P. were associated with investigation - experimental performance, writing – review, editing, and revision. D.M., J.G., and K.M. were associated with investigation, writing – original draft, writing – review, editing, and revision. N.G.-L. was associated with conceptualization, investigation – study design, writing – original draft, writing – review, editing, and revision.

DISCLOSURE

The authors declare no conflict of interest.

ORCID

Nardhy Gomez-Lopez https://orcid.org/0000-0002-3406-5262

REFERENCES

1. Croy BA, Murphy SP. Maternal-fetal immunology. *Immunol Invest*. 2008;37:389-394.
2. Chaouat G, Petitbarat M, Dubanchet S, Rahmati M, Ledee N. Tolerance to the foetal allograft?. *Am J Reprod Immunol*. 2010;63:624-636.
3. Arck PC, Hecher K. Fetomaternal immune cross-talk and its consequences for maternal and offspring's health. *Nat Med*. 2013;19: 548-556.
4. Erlebacher A. Immunology of the maternal-fetal interface. *Annu Rev Immunol*. 2013;31:387-411.
5. Bonney EA. Alternative theories: pregnancy and immune tolerance. *J Reprod Immunol*. 2017;123:65-71.
6. Petroff MG. Immune interactions at the maternal-fetal interface. *J Reprod Immunol*. 2005;68:1-13.
7. Robertson SA, Guerin LR, Bromfield JJ, Branson KM, Ahlstrom AC, Care AS. Seminal fluid drives expansion of the CD4+CD25+ T regulatory cell pool and induces tolerance to paternal alloantigens in mice. *Biol Reprod*. 2009;80:1036-1045.
8. Robertson SA, Guerin LR, Moldenhauer LM, Hayball JD. Activating T regulatory cells for tolerance in early pregnancy - the contribution of seminal fluid. *J Reprod Immunol*. 2009;83:109-116.
9. Moldenhauer LM, Diener KR, Thring DM, Brown MP, Hayball JD, Robertson SA. Cross-presentation of male seminal fluid antigens elicits T cell activation to initiate the female immune response to pregnancy. *J Immunol*. 2009;182:8080-8093.
10. Guerin LR, Moldenhauer LM, Prins JR, Bromfield JJ, Hayball JD, Robertson SA. Seminal fluid regulates accumulation of FOXP3+ regulatory T cells in the preimplantation mouse uterus through expanding the FOXP3+ cell pool and CCL19-mediated recruitment. *Biol Reprod*. 2011;85:397-408.
11. Sharkey DJ, Tremellen KP, Jasper MJ, Gemzell-Danielsson K, Robertson SA. Seminal fluid induces leukocyte recruitment and cytokine and chemokine mRNA expression in the human cervix after coitus. *J Immunol*. 2012;188:2445-2454.
12. Saito S, Shima T, Nakashima A, Inada K, Yoshino O. Role of paternal antigen-specific treg cells in successful implantation. *Am J Reprod Immunol*. 2016;75:310-316.
13. Moldenhauer LM, Schjenken JE, Hope CM, et al. Thymus-derived regulatory t cells exhibit foxp3 epigenetic modification and phenotype attenuation after mating in mice. *J Immunol*. 2019;203:647-657.
14. Shima T, Nakashima A, Yasuda I, et al. Uterine CD11c+ cells induce the development of paternal antigen-specific Tregs via seminal plasma priming. *J Reprod Immunol*. 2020:103165.
15. Hill JA. Immunological mechanisms of pregnancy maintenance and failure: a critique of theories and therapy. *Am J Reprod Immunol*. 1990;22:33-41.
16. Tafuri A, Alferink J, Moller P, Hammerling GJ, Arnold B. T cell awareness of paternal alloantigens during pregnancy. *Science*. 1995;270:630-633.
17. Petroff MG. Review: fetal antigens–identity, origins, and influences on the maternal immune system. *Placenta*. 2011;32:S176-181. Suppl.
18. Chaouat G, Voisin GA, Escalier D, Robert P. Facilitation reaction (enhancing antibodies and suppressor cells) and rejection reaction (sensitized cells) from the mother to the paternal antigens of the conceptus. *Clin Exp Immunol*. 1979;35:13-24.
19. Aluvihare VR, Kallikourdis M, Betz AG. Regulatory T cells mediate maternal tolerance to the fetus. *Nat Immunol*. 2004;5:266-271.
20. Sasaki Y, Sakai M, Miyazaki S, Higuma S, Shiozaki A, Saito S. Decidual and peripheral blood CD4+CD25+ regulatory T cells in early pregnancy subjects and spontaneous abortion cases. *Mol Hum Reprod*. 2004;10:347-353.

21. Heikkinen J, Mottonen M, Alanen A, Lassila O. Phenotypic characterization of regulatory T cells in the human decidua. *Clin Exp Immunol*. 2004;136:373-378.
22. Zenclussen AC, Gerlof K, Zenclussen ML, et al. Abnormal T-cell reactivity against paternal antigens in spontaneous abortion: adoptive transfer of pregnancy-induced CD4+CD25+ T regulatory cells prevents fetal rejection in a murine abortion model. *Am J Pathol*. 2005;166:811-822.
23. Kahn DA, Baltimore D. Pregnancy induces a fetal antigen-specific maternal T regulatory cell response that contributes to tolerance. *Proc Natl Acad Sci U S A*. 2010;107:9299-9304.
24. Shima T, Sasaki Y, Itoh M, et al. Regulatory T cells are necessary for implantation and maintenance of early pregnancy but not late pregnancy in allogeneic mice. *J Reprod Immunol*. 2010;85:121-129.
25. Samstein RM, Josefowicz SZ, Arvey A, Treuting PM, Rudensky AY. Extrathymic generation of regulatory T cells in placental mammals mitigates maternal-fetal conflict. *Cell*. 2012;150:29-38.
26. Rowe JH, Ertelt JM, Xin L, Way SS. Pregnancy imprints regulatory memory that sustains anergy to fetal antigen. *Nature*. 2012;490:102-106.
27. Shima T, Inada K, Nakashima A, et al. Paternal antigen-specific proliferating regulatory T cells are increased in uterine-draining lymph nodes just before implantation and in pregnant uterus just after implantation by seminal plasma-priming in allogeneic mouse pregnancy. *J Reprod Immunol*. 2015;108:72-82.
28. van der Zwan A, Bi K, Norwitz ER, et al. Mixed signature of activation and dysfunction allows human decidual CD8(+) T cells to provide both tolerance and immunity. *Proc Natl Acad Sci U S A*. 2018;115:385-390.
29. Slutsky R, Romero R, Xu Y, et al. Exhausted and senescent T cells at the maternal-fetal interface in preterm and term labor. *J Immunol Res*. 2019;2019:3128010.
30. Hunt JS, Manning LS, Wood GW. Macrophages in murine uterus are immunosuppressive. *Cell Immunol*. 1984;85:499-510.
31. Tawfik OW, Hunt JS, Wood GW. Partial characterization of uterine cells responsible for suppression of murine maternal anti-fetal immune responses. *J Reprod Immunol*. 1986;9:213-224.
32. Gustafsson C, Mjosberg J, Matussek A, et al. Gene expression profiling of human decidual macrophages: evidence for immunosuppressive phenotype. *PLoS One*. 2008;3:e2078.
33. Repnik U, Tilburgs T, Roelen DL, et al. Comparison of macrophage phenotype between decidua basalis and decidua parietalis by flow cytometry. *Placenta*. 2008;29:405-412.
34. Svensson J, Jenmalm MC, Matussek A, Geffers R, Berg G, Ernerudh J. Macrophages at the fetal-maternal interface express markers of alternative activation and are induced by M-CSF and IL-10. *J Immunol*. 2011;187:3671-3682.
35. Houser BL, Tilburgs T, Hill J, Nicotra ML, Strominger JL. Two unique human decidual macrophage populations. *J Immunol*. 2011;186:2633-2642.
36. Miller D, Motomura K, Garcia-Flores V, Romero R, Gomez-Lopez N. Innate lymphoid cells in the maternal and fetal compartments. *Front Immunol*. 2018;9:2396.
37. Mendes J, Areia AL, Rodrigues-Santos P, Santos-Rosa M, Mota-Pinto A, Innate lymphoid cells in human pregnancy. *Front Immunol* 2020;11:551707.
38. Ellis SA, Sargent IL, Redman CW, McMichael AJ. Evidence for a novel HLA antigen found on human extravillous trophoblast and a choriocarcinoma cell line. *Immunology*. 1986;59:595-601.
39. Kovats S, Main EK, Librach C, Stubblebine M, Fisher SJ, DeMars R. A class I antigen, HLA-G, expressed in human trophoblasts. *Science*. 1990;248:220-223.
40. Chumbley G, King A, Robertson K, Holmes N, Loke YW. Resistance of HLA-G and HLA-A2 transfectants to lysis by decidual NK cells. *Cell Immunol*. 1994;155:312-322.
41. Vento-Tormo R, Efremova M, Botting RA, et al. Single-cell reconstruction of the early maternal-fetal interface in humans. *Nature*. 2018;563:347-353.
42. Zhang YH, Aldo P, You Y, et al. Trophoblast-secreted soluble-PD-L1 modulates macrophage polarization and function. *J Leukoc Biol*. 2020;108:983-998.
43. PrabhuDas M, Bonney E, Caron K, et al. Immune mechanisms at the maternal-fetal interface: perspectives and challenges. *Nat Immunol*. 2015;16:328-334.
44. Herzenberg LA, Bianchi DW, Schroder J, Cann HM, Iverson GM. Fetal cells in the blood of pregnant women: detection and enrichment by fluorescence-activated cell sorting. *Proc Natl Acad Sci U S A*. 1979;76:1453-1455.
45. Bianchi DW, Zickwolf GK, Weil GJ, Sylvester S, DeMaria MA. Male fetal progenitor cells persist in maternal blood for as long as 27 years postpartum. *Proc Natl Acad Sci U S A*. 1996;93:705-708.
46. Ariga H, Ohto H, Busch MP, et al. Kinetics of fetal cellular and cell-free DNA in the maternal circulation during and after pregnancy: implications for noninvasive prenatal diagnosis. *Transfusion*. 2001;41:1524-1530.
47. Maloney S, Smith A, Furst DE, et al. Microchimerism of maternal origin persists into adult life. *J Clin Invest*. 1999;104:41-47.
48. Srivatsa B, Srivatsa S, Johnson KL, Bianchi DW. Maternal cell microchimerism in newborn tissues. *J Pediatr*. 2003;142:31-35.
49. Su EC, Johnson KL, Tighiouart H, Bianchi DW. Murine maternal cell microchimerism: analysis using real-time PCR and in vivo imaging. *Biol Reprod*. 2008;78:883-887.
50. Stevens AM, Hermes HM, Kiefer MM, Rutledge JC, Nelson JL. Chimeric maternal cells with tissue-specific antigen expression and morphology are common in infant tissues. *Pediatr Dev Pathol*. 2009;12:337-346.
51. Kinder JM, Stelzer IA, Arck PC, Way SS. Immunological implications of pregnancy-induced microchimerism. *Nat Rev Immunol*. 2017;17:483-494.
52. Cheng SB, Davis S, Sharma S. Maternal-fetal cross talk through cell-free fetal DNA, telomere shortening, microchimerism, and inflammation. *Am J Reprod Immunol*. 2018;79:e12851.
53. Knight M, Redman CW, Linton EA, Sargent IL. Shedding of syncytiotrophoblast microvilli into the maternal circulation in pre-eclamptic pregnancies. *Br J Obstet Gynaecol*. 1998;105:632-640.
54. Sabapatha A, Gercel-Taylor C, Taylor DD. Specific isolation of placenta-derived exosomes from the circulation of pregnant women and their immunoregulatory consequences. *Am J Reprod Immunol*. 2006;56:345-355.
55. Redman CW, Sargent IL. Microparticles and immunomodulation in pregnancy and pre-eclampsia. *J Reprod Immunol*. 2007;76:61-67.
56. Germain SJ, Sacks GP, Sooranna SR, Sargent IL, Redman CW. Systemic inflammatory priming in normal pregnancy and preeclampsia: the role of circulating syncytiotrophoblast microparticles. *J Immunol*. 2007;178:5949-5956.
57. Burton GJ, Jones CJ. Syncytial knots, sprouts, apoptosis, and trophoblast deportation from the human placenta. *Taiwan J Obstet Gynecol*. 2009;48:28-37.
58. Holland OJ, Linscheid C, Hodes HC, et al. Minor histocompatibility antigens are expressed in syncytiotrophoblast and trophoblast debris: implications for maternal alloreactivity to the fetus. *Am J Pathol*. 2012;180:256-266.
59. Stenqvist AC, Nagaeva O, Baranov V, Mincheva-Nilsson L. Exosomes secreted by human placenta carry functional Fas ligand and TRAIL molecules and convey apoptosis in activated immune cells, suggesting exosome-mediated immune privilege of the fetus. *J Immunol*. 2013;191:5515-5523.
60. Gohner C, Plosch T, Faas MM. Immune-modulatory effects of syncytiotrophoblast extracellular vesicles in pregnancy and preeclampsia. *Placenta*. 2017:S41. Suppl.

61. Familari M, Cronqvist T, Masoumi Z, Hansson SR. Placenta-derived extracellular vesicles: their cargo and possible functions. *Reprod Fertil Dev*. 2017;29:433-447.
62. Tong M, Abrahams VM, Chamley LW. Immunological effects of placental extracellular vesicles. *Immunol Cell Biol*. 2018.
63. Nair S, Salomon C. Extracellular vesicles and their immunomodulatory functions in pregnancy. *Semin Immunopathol*. 2018;40:425-437.
64. Reddy A, Zhong XY, Rusterholz C, et al. The effect of labour and placental separation on the shedding of syncytiotrophoblast microparticles, cell-free DNA and mRNA in normal pregnancy and pre-eclampsia. *Placenta*. 2008;29:942-949.
65. Kshirsagar SK, Alam SM, Jasti S, et al. Immunomodulatory molecules are released from the first trimester and term placenta via exosomes. *Placenta*. 2012;33:982-990.
66. Tannetta DS, Dragovic RA, Gardiner C, Redman CW, Sargent IL. Characterisation of syncytiotrophoblast vesicles in normal pregnancy and pre-eclampsia: expression of Flt-1 and endoglin. *PLoS One*. 2013;8:e56754.
67. Kovacs AF, Fekete N, Turiak L, et al. Unravelling the role of trophoblastic-derived extracellular vesicles in regulatory T cell differentiation. *Int J Mol Sci*. 2019;20.
68. Tannetta D, Collett G, Vatish M, Redman C, Sargent I. Syncytiotrophoblast extracellular vesicles - Circulating biopsies reflecting placental health. *Placenta*. 2017;52:134-138.
69. Sacks GP, Studena K, Sargent K, Redman CW. Normal pregnancy and preeclampsia both produce inflammatory changes in peripheral blood leukocytes akin to those of sepsis. *Am J Obstet Gynecol*. 1998;179:80-86.
70. Naccasha N, Gervasi MT, Chaiworapongsa T, et al. Phenotypic and metabolic characteristics of monocytes and granulocytes in normal pregnancy and maternal infection. *Am J Obstet Gynecol*. 2001;185:1118-1123.
71. Gomez-Lopez N, Tanaka S, Zaeem Z, Metz GA, Olson DM. Maternal circulating leukocytes display early chemotactic responsiveness during late gestation. *BMC Pregnancy Childbirth*. 2013;13 Suppl 1:S8
72. Kindzelskii AL, Ueki T, Michibata H, Chaiworapongsa T, Romero R, Petty HR. 6-phosphogluconate dehydrogenase and glucose-6-phosphate dehydrogenase form a supramolecular complex in human neutrophils that undergoes retrograde trafficking during pregnancy. *J Immunol*. 2004;172:6373-6381.
73. Kindzelskii AL, Clark AJ, Espinoza J, et al. Myeloperoxidase accumulates at the neutrophil surface and enhances cell metabolism and oxidant release during pregnancy. *Eur J Immunol*. 2006;36:1619-1628.
74. Persellin RH, Thoi LL. Human polymorphonuclear leukocyte phagocytosis in pregnancy. Development of inhibition during gestation and recovery in the postpartum period. *Am J Obstet Gynecol*. 1979;134:250-255.
75. Lampe R, Kover A, Szucs S, et al. Phagocytic index of neutrophil granulocytes and monocytes in healthy and preeclamptic pregnancy. *J Reprod Immunol*. 2015;107:26-30.
76. Barriga C, Rodriguez AB, Ortega E. Increased phagocytic activity of polymorphonuclear leukocytes during pregnancy. *Eur J Obstet Gynecol Reprod Biol*. 1994;57:43-46.
77. Luppi P, Haluszczak C, Betters D, Richard CA, Trucco M, DeLoia JA. Monocytes are progressively activated in the circulation of pregnant women. *J Leukoc Biol*. 2002;72:874-884.
78. Pflitsch C, Feldmann CN, Richert L, et al. In-depth characterization of monocyte subsets during the course of healthy pregnancy. *J Reprod Immunol*. 2020;141:103151.
79. Sacks GP, Redman CW, Sargent IL. Monocytes are primed to produce the Th1 type cytokine IL-12 in normal human pregnancy: an intracellular flow cytometric analysis of peripheral blood mononuclear cells. *Clin Exp Immunol*. 2003;131:490-497.
80. Koumandakis E, Koumandaki I, Kaklamani E, Sparos L, Aravantinos D, Trichopoulos D. Enhanced phagocytosis of mononuclear phagocytes in pregnancy. *Br J Obstet Gynaecol*. 1986;93:1150-1154.
81. Erlebacher A, Vencato D, Price KA, Zhang D, Glimcher LH. Constraints in antigen presentation severely restrict T cell recognition of the allogeneic fetus. *J Clin Invest*. 2007;117:1399-1411.
82. Moldenhauer LM, Hayball JD, Robertson SA. Utilising T cell receptor transgenic mice to define mechanisms of maternal T cell tolerance in pregnancy. *J Reprod Immunol*. 2010;87:1-13.
83. Petroff MG. Review: fetal antigens–identity, origins, and influences on the maternal immune system. *Placenta*. 2011;32 Suppl 2:S176-181.
84. Arenas-Hernandez M, Sanchez-Rodriguez EN, Mial TN, Robertson SA, Gomez-Lopez N. Isolation of leukocytes from the murine tissues at the maternal-fetal interface. *J Vis Exp*. 2015:e52866.
85. Gomez-Lopez N, Romero R, Schwenkel G, et al. Cell-Free fetal DNA increases prior to labor at term and in a subset of preterm births. *Reprod Sci*. 2020;27:218-232.
86. Straszewski-Chavez SL, Abrahams VM, Alvero AB, et al. The isolation and characterization of a novel telomerase immortalized first trimester trophoblast cell line, Swan 71. *Placenta*. 2009;30:939-948.
87. Jain CV, Kadam L, van Dijk M, et al. Fetal genome profiling at 5 weeks of gestation after noninvasive isolation of trophoblast cells from the endocervical canal. *Sci Transl Med*. 2016;8:363re364.
88. Moser G, Drewlo S, Huppertz B, Armant DR. Trophoblast retrieval and isolation from the cervix: origins of cervical trophoblasts and their potential value for risk assessment of ongoing pregnancies. *Hum Reprod Update*. 2018;24:484-496.
89. Todd RF 3rd, Nadler LM, Schlossman SF. Antigens on human monocytes identified by monoclonal antibodies. *J Immunol*. 1981;126:1435-1442.
90. Chen HM, Pahl HL, Scheibe RJ, Zhang DE, Tenen DG. The Sp1 transcription factor binds the CD11b promoter specifically in myeloid cells in vivo and is essential for myeloid-specific promoter activity. *J Biol Chem*. 1993;268:8230-8239.
91. Gustafson MP, Lin Y, Maas ML, et al. A method for identification and analysis of non-overlapping myeloid immunophenotypes in humans. *PLoS One*. 2015;10:e0121546.
92. Rosen H, Gordon S. Monoclonal antibody to the murine type 3 complement receptor inhibits adhesion of myelomonocytic cells in vitro and inflammatory cell recruitment in vivo. *J Exp Med*. 1987;166:1685-1701.
93. Jutila MA, Rott L, Berg EL, Butcher EC. Function and regulation of the neutrophil MEL-14 antigen in vivo: comparison with LFA-1 and MAC-1. *J Immunol*. 1989;143:3318-3324.
94. Roche PA, Furuta K. The ins and outs of MHC class II-mediated antigen processing and presentation. *Nat Rev Immunol*. 2015;15:203-216.
95. Chen L, Flies DB. Molecular mechanisms of T cell co-stimulation and co-inhibition. *Nat Rev Immunol*. 2013;13:227-242.
96. Ezekowitz RA, Sastry K, Bailly P, Warner A. Molecular characterization of the human macrophage mannose receptor: demonstration of multiple carbohydrate recognition-like domains and phagocytosis of yeasts in Cos-1 cells. *J Exp Med*. 1990;172:1785-1794.
97. Cuartero MI, Ballesteros I, Moraga A, et al. A. N2 neutrophils, novel players in brain inflammation after stroke: modulation by the PPARgamma agonist rosiglitazone. *Stroke*. 2013;44:3498-3508.
98. Nielsen MC, Andersen MN, Rittig N, et al. The macrophage-related biomarkers sCD163 and sCD206 are released by different shedding mechanisms. *J Leukoc Biol*. 2019;106:1129-1138.
99. Ono Y, Yoshino O, Hiraoka T, et al. CD206+ M2-Like macrophages are essential for successful implantation. *Front Immunol*. 2020;11:557184.

100. Simon SI, Burns AR, Taylor AD, et al. L-selectin (CD62L) cross-linking signals neutrophil adhesive functions via the Mac-1 (CD11b/CD18) beta 2-integrin. *J Immunol*. 1995;155:1502-1514.
101. Leon B, Ardavin C. Monocyte migration to inflamed skin and lymph nodes is differentially controlled by L-selectin and PSGL-1. *Blood*. 2008;111:3126-3130.
102. Bjorkman L, Christenson K, Davidsson L, et al. Neutrophil recruitment to inflamed joints can occur without cellular priming. *J Leukoc Biol*. 2019;105:1123-1130.
103. Chadwick JW, Fine N, Khoury W, et al. Tissue-specific murine neutrophil activation states in health and inflammation. *J Leukoc Biol*. 2020.
104. Atay S, Gercel-Taylor C, Kesimer M, Taylor DD. Morphologic and proteomic characterization of exosomes released by cultured extravillous trophoblast cells. *Exp Cell Res*. 2011;317:1192-1202.
105. Alam SMK, Jasti S, Kshirsagar SK, et al, Trophoblast glycoprotein (tpgb/5t4) in human placenta: expression, regulation, and presence in extracellular microvesicles and exosomes. *Reprod Sci* 2018;25: 185-197.
106. Delorme-Axford E, Donker RB, Mouillet JF, et al. Human placental trophoblasts confer viral resistance to recipient cells. *Proc Natl Acad Sci U S A*. 2013;110:12048-12053.
107. Delorme-Axford E, Bayer A, Sadovsky Y, Coyne CB. Autophagy as a mechanism of antiviral defense at the maternal-fetal interface. *Autophagy*. 2013;9:2173-2174.
108. Bayer A, Lennemann NJ, Ouyang Y, et al. Type III interferons produced by human placental trophoblasts confer protection against zika virus infection. *Cell Host Microbe*. 2016;19:705-712.
109. Arora N, Sadovsky Y, Dermody TS, Coyne CB. Microbial vertical transmission during human pregnancy. *Cell Host Microbe*. 2017;21:561-567.
110. Megli C, Morosky S, Rajasundaram D, Coyne CB. Inflammasome signaling in human placental trophoblasts regulates immune defense against Listeria monocytogenes infection. *J Exp Med*. 2021;218.
111. Simister NE, Story CM, Chen HL, Hunt JS. An IgG-transporting Fc receptor expressed in the syncytiotrophoblast of human placenta. *Eur J Immunol*. 1996;26:1527-1531.
112. Firan M, Bawdon R, Radu C, et al. The MHC class I-related receptor, FcRn, plays an essential role in the maternofetal transfer of gamma-globulin in humans. *Int Immunol*. 2001;13:993-1002.
113. Radulescu L, Antohe F, Jinga V, Ghetie V, Simionescu M. Neonatal Fc receptors discriminates and monitors the pathway of native and modified immunoglobulin G in placental endothelial cells. *Hum Immunol*. 2004;65:578-585.
114. Palmeira P, Costa-Carvalho BT, Arslanian C, Pontes GN, Nagao AT, Carneiro-Sampaio MM. Transfer of antibodies across the placenta and in breast milk from mothers on intravenous immunoglobulin. *Pediatr Allergy Immunol*. 2009;20:528-535.
115. Palmeira P, Quinello C, Silveira-Lessa AL, Zago CA, Carneiro-Sampaio M. IgG placental transfer in healthy and pathological pregnancies. *Clin Dev Immunol*. 2012;2012:985646.
116. Lo YM, Lo ES, Watson N, et al. Two-way cell traffic between mother and fetus: biologic and clinical implications. *Blood*. 1996;88:4390-4395.
117. Lapaire O, Holzgreve W, Oosterwijk JC, Brinkhaus R, Bianchi DW. Georg Schmorl on trophoblasts in the maternal circulation. *Placenta*. 2007;28:1-5.
118. Redman CW, Sargent IL. Circulating microparticles in normal pregnancy and pre-eclampsia. *Placenta*. 2008;29:S73-77.
119. Jeanty C, Derderian SC, Mackenzie TC. Maternal-fetal cellular trafficking: clinical implications and consequences. *Curr Opin Pediatr*. 2014;26:377-382.
120. Lo YM, Corbetta N, Chamberlain PF, et al. Presence of fetal DNA in maternal plasma and serum. *Lancet*. 1997;350:485-487.
121. Lo YM, Tein MS, Lau TK, et al. Quantitative analysis of fetal DNA in maternal plasma and serum: implications for noninvasive prenatal diagnosis. *Am J Hum Genet*. 1998;62:768-775.
122. Khosrotehrani K, Wataganara T, Bianchi DW, Johnson KL. Fetal cell-free DNA circulates in the plasma of pregnant mice: relevance for animal models of fetomaternal trafficking. *Hum Reprod*. 2004;19:2460-2464.
123. Taglauer ES, Wilkins-Haug L, Bianchi DW. Review: cell-free fetal DNA in the maternal circulation as an indication of placental health and disease. *Placenta*. 2014:S64-68. Suppl.
124. Herrera CA, Stoerker J, Carlquist J, et al. Cell-free DNA, inflammation, and the initiation of spontaneous term labor. *Am J Obstet Gynecol*. 2017;217:583 e581-583 e588.
125. Belo L, Santos-Silva A, Rocha S, et al. Rebelo, I. Fluctuations in C-reactive protein concentration and neutrophil activation during normal human pregnancy. *Eur J Obstet Gynecol Reprod Biol*. 2005;123: 46-51.
126. Veenstra van Nieuwenhoven AL, Bouman A, Moes H, et al. Endotoxin-induced cytokine production of monocytes of third-trimester pregnant women compared with women in the follicular phase of the menstrual cycle. *Am J Obstet Gynecol*. 2003;188:1073-1077.
127. Kraus TA, Engel SM, Sperling RS, et al. Characterizing the pregnancy immune phenotype: results of the viral immunity and pregnancy (VIP) study. *J Clin Immunol*. 2012;32:300-311.
128. Kostlin N, Kugel H, Spring B, et al. Granulocytic myeloid derived suppressor cells expand in human pregnancy and modulate T-cell responses. *Eur J Immunol*. 2014;44:2582-2591.
129. Pan T, Liu Y, Zhong LM, et al. Myeloid-derived suppressor cells are essential for maintaining feto-maternal immunotolerance via STAT3 signaling in mice. *J Leukoc Biol*. 2016;100:499-511.
130. Ostrand-Rosenberg S, Sinha P, Figley C, et al. Frontline Science: myeloid-derived suppressor cells (MDSCs) facilitate maternal-fetal tolerance in mice. *J Leukoc Biol*. 2017;101:1091-1101.
131. Aghaeepour N, Ganio EA, McIlwain D, et al. An immune clock of human pregnancy. *Sci Immunol*. 2017;2.
132. Gomez-Lopez N, Laresgoiti-Servitje E, Olson DM, Estrada-Gutierrez G, Vadillo-Ortega F. The role of chemokines in term and premature rupture of the fetal membranes: a review. *Biol Reprod*. 2010;82: 809-814.
133. Gomez-Lopez N, Vadillo-Perez L, Nessim S, Olson DM, Vadillo-Ortega F. Choriodecidua and amnion exhibit selective leukocyte chemotaxis during term human labor. *Am J Obstet Gynecol*. 2011;204:364 e369-316.
134. Gomez-Lopez N, Olson D, (2012) Leukocyte activation and methods of use thereof. (USPTO, ed) The Governors of the University of Alberta, United States.
135. Gomez-Lopez N, Tong WC, Arenas-Hernandez M, et al. Chemotactic activity of gestational tissues through late pregnancy, term labor, and RU486-induced preterm labor in Guinea pigs. *Am J Reprod Immunol*. 2015;73:341-352.
136. Giaglis S, Stoikou M, Sur Chowdhury C, et al. Multimodal regulation of NET formation in pregnancy: Progesterone antagonizes the pro-NETotic effect of estrogen and G-CSF. *Front Immunol*. 2016;7: 565.
137. Gosselin EJ, Wardwell K, Rigby WF, Guyre PM. Induction of MHC class II on human polymorphonuclear neutrophils by granulocyte/macrophage colony-stimulating factor, IFN-gamma, and IL-3. *J Immunol*. 1993;151:1482-1490.
138. Windhagen A, Maniak S, Gebert A, Ferger I, Wurster U, Heidenreich F. Human polymorphonuclear neutrophils express a B7-1-like molecule. *J Leukoc Biol*. 1999;66:945-952.
139. Meinderts SM, Baker G, van Wijk S, et al. Neutrophils acquire antigen-presenting cell features after phagocytosis of IgG-opsonized erythrocytes. *Blood Adv*. 2019;3:1761-1773.

140. Vono M, Lin A, Norrby-Teglund A, Koup RA, Liang F, Lore K. Neutrophils acquire the capacity for antigen presentation to memory CD4(+) T cells in vitro and ex vivo. *Blood*. 2017;129:1991-2001.
141. Silvestre-Roig C, Hidalgo A, Soehnlein O. Neutrophil heterogeneity: implications for homeostasis and pathogenesis. *Blood*. 2016;127:2173-2181.
142. Giese MA, Hind LE, Huttenlocher A. Neutrophil plasticity in the tumor microenvironment. *Blood*. 2019;133:2159-2167.
143. Bouchery T, Harris N. Neutrophil-macrophage cooperation and its impact on tissue repair. *Immunol Cell Biol*. 2019;97:289-298.
144. Nadkarni S, Smith J, Sferruzzi-Perri AN, et al. Neutrophils induce proangiogenic T cells with a regulatory phenotype in pregnancy. *Proc Natl Acad Sci U S A*. 2016;113:E8415.
145. Jakubzick CV, Randolph GJ, Henson PM. Monocyte differentiation and antigen-presenting functions. *Nat Rev Immunol*. 2017;17:349-362.
146. Apps R, Kotliarov Y, Cheung F, et al. Multimodal immune phenotyping of maternal peripheral blood in normal human pregnancy. *JCI Insight*. 2020;5.
147. Han X, Ghaemi MS, Ando K, et al. Differential dynamics of the maternal immune system in healthy pregnancy and preeclampsia. *Front Immunol*. 2019;10:1305.
148. Pique-Regi R, Romero R, Tarca AL, et al. Single cell transcriptional signatures of the human placenta in term and preterm parturition. *Elife*. 2019;8.
149. Hunt JS, Robertson SA. Uterine macrophages and environmental programming for pregnancy success. *J Reprod Immunol*. 1996;32:1-25.
150. Cohen PE, Nishimura K, Zhu L, Pollard JW. Macrophages: important accessory cells for reproductive function. *J Leukoc Biol*. 1999;66:765-772.
151. Care AS, Diener KR, Jasper MJ, Brown HM, Ingman WV, Robertson SA. Macrophages regulate corpus luteum development during embryo implantation in mice. *J Clin Invest*. 2013;123:3472-3487.
152. Qiu X, Zhu L, Pollard JW. Colony-stimulating factor-1-dependent macrophage functions regulate the maternal decidua immune responses against Listeria monocytogenes infections during early gestation in mice. *Infect Immun*. 2009;77:85-97.
153. Svensson-Arvelund J, Mehta RB, Lindau R, et al. The human fetal placenta promotes tolerance against the semiallogeneic fetus by inducing regulatory T cells and homeostatic M2 macrophages. *J Immunol*. 2015;194:1534-1544.
154. Xu Y, Romero R, Miller D, et al. An M1-like macrophage polarization in decidual tissue during spontaneous preterm labor that is attenuated by rosiglitazone treatment. *J Immunol*. 2016;196:2476-2491.
155. Gomez-Lopez N, Garcia-Flores V, Chin PY, et al. Macrophages exert homeostatic actions in pregnancy to protect against preterm birth and fetal inflammatory injury. *JCI Insight*. 2021. In Press.
156. Garcia-Flores V, Romero R, Schwenkel G, Hassan SS, Gomez-Lopez N. A cellular regenerative approach to prevent preterm birth: in vitro M2-polarized macrophages. *Reprod Sci*. 2019;26:74A.
157. Garcia-Flores V, Romero R, Xu Y, et al. M2-polarized macrophages as a potential cell therapy to mitigate inflammation-induced preterm birth. *J Immunol*. 2020;204:145.115.
158. Gamliel M, Goldman-Wohl D, Isaacson B, et al. Trained memory of human uterine nk cells enhances their function in subsequent pregnancies. *Immunity*. 2018;48:951-962 e955.
159. Dominguez-Andres J, Netea MG. Long-term reprogramming of the innate immune system. *J Leukoc Biol*. 2019;105:329-338.
160. Gomez-Lopez N, Arenas-Hernandez M, Romero R, et al. Regulatory T cells play a role in a subset of idiopathic preterm labor/birth and adverse neonatal outcomes. *Cell Rep*. 2020;32:107874.
161. Ersland K, Wüthrich M, Klein BS. Dynamic interplay among monocyte-derived, dermal, and resident lymph node dendritic cells during the generation of vaccine immunity to fungi. *Cell Host Microbe*. 2010;7:474-487.
162. Samstein M, Schreiber HA, Leiner IM, Susac B, Glickman MS, Pamer EG. Essential yet limited role for $CCR2^{+}$ inflammatory monocytes during Mycobacterium tuberculosis-specific T cell priming. *Elife*. 2013;2:e01086.
163. Schreiber HA, Loschko J, Karssemeijer RA, et al. Intestinal monocytes and macrophages are required for T cell polarization in response to citrobacter rodentium. *J Exp Med*. 2013;210:2025-2039.

SUPPORTING INFORMATION

Additional supporting information may be found in the online version of the article at the publisher's website.

How to cite this article: Arenas-Hernandez M, Romero R, Gershater M, et al. Specific innate immune cells uptake fetal antigen and display homeostatic phenotypes in the maternal circulation. *J Leukoc Biol*. 2022;111:519–538. https://doi.org/10.1002/JLB.5HI0321-179RR